EXPERIMENTAL INVESTIGATION ON CONCENTRICALLY LOADED SQUARE CONCRETE-FILLED STEEL TUBULAR COLUMNS

MD. MOFIZUL ISLAM

MASTER OF SCIENCE IN CIVIL ENGINERING (STRUCTURAL)

DEPARTMENT OF CIVIL ENGINEERING

BANGLADESH UNIVERSITY OF ENGINEERING AND TECHNOLOGY

DHAKA, BANGLADESH

MARCH 2019

EXPERIMENTAL INVESTIGATION ON CONCENTRICALLY LOADED SQUARE CONCRETE-FILLED STEEL TUBULAR COLUMNS

by

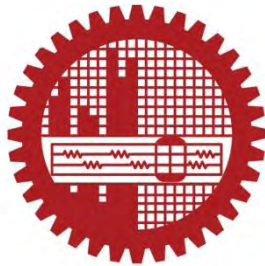**MD. MOFIZUL ISLAM**

Student No: 0417042355F

A thesis submitted to the Department of Civil Engineering of Bangladesh University of Engineering and Technology, Dhaka in partial fulfillment of the requirement for the degree of

MASTER OF SCIENCE IN CIVIL ENGINERING (STRUCTURAL)

DEPARTMENT OF CIVIL ENGINEERING

BANGLADESH UNIVERSITY OF ENGINEERING AND TECHNOLOGY

DHAKA, BANGLADESH

MARCH 2019

CERTIFICATE OF APPROVAL

The thesis titled **"Experimental Investigation on Concentrically Loaded Square Concrete-Filled Steel Tubular Columns"** submitted by Md. Mofizul Islam, Student Number: 0417042355F, Session: April, 2017 has been accepted as satisfactory in partial fulfillment of the requirement for the degree of Master of Science in Civil Engineering (Structural) on 25th March, 2019.
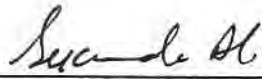
BOARD OF EXAMINERS

1. **Dr. Mahbuba Begum**
   Professor
   Department of Civil Engineering
   BUET, Dhaka-1000

   Chairman
   (Supervisor)

2. **Dr. Ahsanul Kabir**
   Professor and Head
   Department of Civil Engineering
   BUET, Dhaka-1000

   Member
   (Ex-Officio)

3. **Dr. Sk. Sekender Ali**
   Professor
   Department of Civil Engineering
   BUET, Dhaka-1000

   Member

4. **Dr. Md. Soebur Rahman**
   Major & Associate Professor
   Department of Civil Engineering
   Military Institute of Science and
   Technology (MIST), Dhaka-1216

   Member
   (External)

Declaration

Except for the contents where specific references have been made to the work of others, the studies embodied in this dissertation are the outcome of the research conducted by the author. No part of this dissertation has been submitted to any other University or other educational establishment for a Degree, Diploma or other qualification (except for publication).

Mofizul Islam

Md. Mofizul Islam

Dedicated

To

My Beloved Parents

ACKNOWLEDGEMENT

ABSTRACT

Concrete filled steel tube (CFST) column consists of a hollow steel tube filled with concrete. This composite section offers numerous structural benefits over reinforced concrete and steel only sections, including high strength, high ductility and large energy absorption capacities. Extensive experimental and numerical studies have been carried out by several researchers on concentrically and eccentrically loaded CFST columns with various geometric and material properties. Most of this research work has been performed on CFST columns constructed with available standard tube shapes. However, limited research has been found on CFST columns in built-up steel sections. Current design rules for CFST columns are specified in AISC-LRFD, ACI 318, EC-4, British standard BS 5400 and Canadian Standard Association CSA. In the upcoming version of Bangladesh National Building Code (BNBC 2016) the design guidelines for CFST columns are included which is adopted from AISC (2005) specifications. The applicability of these design provisions in the construction environment of Bangladesh needs to be explored. To this end, an attempt has been made in this study to investigate the behaviour and strength of the CFST columns constructed with built-up steel section and locally available materials.

This paper presents an experimental investigation on the behavior of CFST columns regarding three parameters: concrete compressive strength, cross sectional slenderness ratio and global slenderness ratio. Total nine CFST columns with square cross section were tested under concentric loading. The tested columns were filled by concrete with compressive strength of 27 MPa to 44 MPa, cross-sectional slenderness ratio of 25 to 42 and global slenderness ratio of 3 to 10. The influence of these parameters on the failure mode, load-strain response, ultimate load and performance indexes of the square CFST column is discussed. Finally, the design approaches adopted in (Eurocode 4, AISC-LRFD 2010, ACI 2014 and Wang et al. 2016) are reviewed and applied to calculate the ultimate strength of the tests columns. Subsequently, the predicted values are compared with the experimental results obtained from the experiments.

Based on the results, it was determined that concrete compressive strength, cross sectional slenderness ratio and global slenderness ratio have significant effect on the fundamental behavior of CFST column. Increasing the concrete compressive strength improved the ultimate capacity and concrete contribution ratio of the column but decreased the peak strain because of its less ductile behavior. On the other hand, columns with higher global slenderness ratio showed lower ultimate capacity and less ductile behavior with global buckling failure. However, columns with lower cross sectional slenderness ratio exhibited better column performance for its higher steel contribution and columns with higher cross sectional slenderness ratio showed outward local buckling failure. Moreover, all the codes somewhat overestimated the capacities except AISC-LRFD (2010). AISC-LRFD (2010) presented best prediction with a mean of 0.99 and Standard deviation of 0.04. EC4 and ACI (2014) predicted higher capacity than the experimental results about 8% and 2% respectively; whilst Wang et al. (2016) predicted highest 12% higher capacity of all the methods analyzed. In general, all the codes showed good agreement with the experimental results.

Table of Contents

Chapter 5 DESIGN CODES AND COMPARISIONS

Chapter 6 CONCLUSIONS AND RECOMMENDATIONS

List of Tables

List of Figures

Notations

RC	Reinforced concrete
CFST	Concrete filled steel tubular column
CFT	Concrete filled tube
HT	Hollow tube
SRC	Steel reinforced concrete
CHS	Circular hollow section
SHS	Square hollow section
RHS	Rectangular hollow section
HST	Hollow steel tube
HPS	High performance steel
CFDST	Concrete filled double skin steel tubular column
B	Width of column
H	Cross-sectional height of column
L	Length of column
T	Thickness of steel
B/t	Column cross-sectional slenderness ratio
L/B	Column global slenderness ratio
OPC	Ordinary Portland cement
UTM	Universal testing machine
LVDT	Linear variable differential transformer
A_s	Area of steel
A_c	Area of concrete
f_u	Ultimate stress
f_c'	Concrete compressive strength
f_y	Yield stress
ε_y	Yield strain
ε_u	Ultimate strain

DI	Ductility index
ξ_s	Steel contribution ratio
P_u	Ultimate load of the tested column
ξ_c	Concrete contribution ratio
α_c	Strength reduction factor
ACI	American Concrete Institute
AISC	American Institute of Steel Construction
EC4	Eurocode 4
AS	Australian code
E_c	Elasticity modulus of concrete
EI_{eff}	Effective stiffness of composite section
E_s	Modulus of elasticity of steel
f_y	Specified minimum yield stress of steel section
f_{ysr}	Specified minimum yield stress of reinforcing bars
K	Effective length factor
L	Laterally unbraced length of the member
W_c	Weight of concrete per unit volume
p_{no}	Nominal compressive strength of axially loaded composite member
p_e	Elastic critical buckling load

CHAPTER 1

INTRODUCTION

1.1   General

Steel-concrete composite construction typically refers to the use of steel and concrete formed together so that the resulting component behaves as a single element. The aim of composite construction is to utilize the best properties of the different materials and to deliver performance that is greater than had the individual components been used together but not unified. Figure 1.1 shows the statistics of using material for the worlds 100 tallest buildings from 1930 to 2015 (Gabel et al. 2015). As can be seen from 1960, all-steel construction has continued to decline as a primary structural material, comprising only 11% of the world's 100 tallest buildings in 2015. Buildings with concrete and composite become the majority of material in construction and the proportions of these two material forms are predicted to increase. Only 3% of buildings which were 200 meters and higher in 2015 were constructed with all-steel material. Without any doubt concrete and composite building construction will be the most popular structural form in the future. The rise of market demand on these materials calls for urgent research.
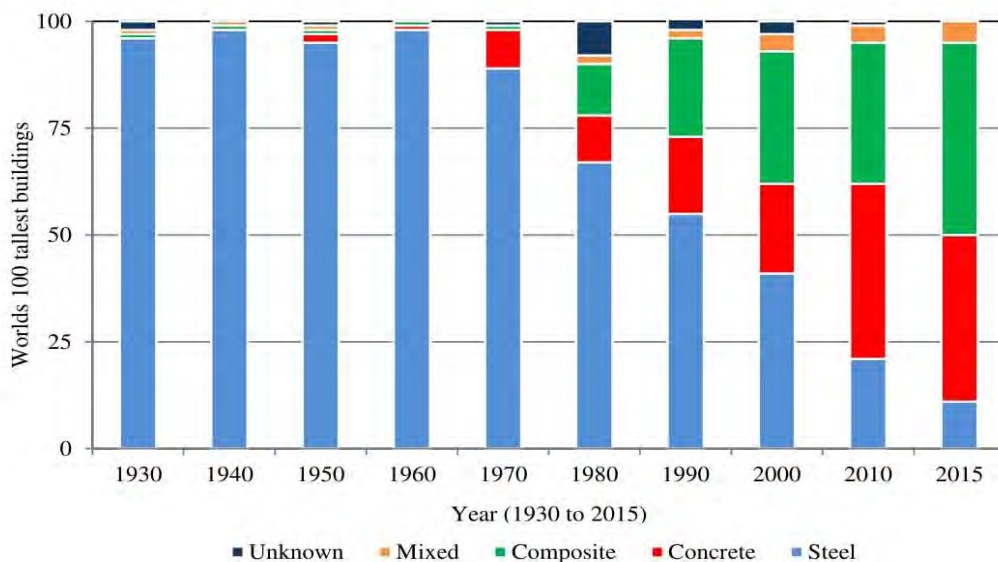
Figure 1.1 World's 100 tallest building's by materials.

In the case of steel and concrete, the best properties would be the tensile capacity of the steel and the compressive capacity of the concrete. A reinforced concrete (RC) structure is a typical application to utilize the advantage of concrete in compression and steel in tension. In addition, a steel-concrete composite structure integrates the respective advantages of both steel and concrete. For example, concrete-filled steel tubes (CFSTs), one of the typical steel-concrete composite structures, combine the full advantages of concrete and steel. Concrete filled steel tube (CFST) column consists of a hollow steel tube filled with concrete. This composite section offers numerous structural benefits over reinforced concrete and steel only sections, including high strength, high ductility and large energy absorption capacities. Performance of different types of columns which have been used in high rise building construction is presented in Table 1.1.

Table 1.1 Performance of different types of columns

Content	RC	Steel	SRC	CFST
Section size	Big	Small	Medium	Small
Seismic behaviour	Fair	Excellent	Good	Excellent
Fire resistance	Excellent	Fair	Excellent	Good
Construction ability	Not good	Excellent	Fair	Excellent
Anti-corrosion	Good	Fair	Excellent	Not bad
Long-term behaviour	Not good	Good	Not bad	Good

During concreting, there is no need for the use of shuttering in CFST structures; hence, the construction cost and time are reduced. In CFST columns the steel tube not only serves as formwork but also provides continuous confinement to concrete core resulting in enhanced strength and ductility of concrete. These advantages have been widely exploited and have led to the extensive use of concrete-filled tubular structures in high rise buildings, bridges and offshore structures (Sakino et al. 2004; Shanmugam and Lakshmi 2001; Susantha et al. 2001).

Figure 1.2 (a) depicts three typical column cross-sections, where the concrete is filled in a circular hollow section (CHS), a square hollow section (SHS) or a rectangular hollow section (RHS), where D and B are the outer dimensions of the steel tube and t is the wall thickness of the tube.
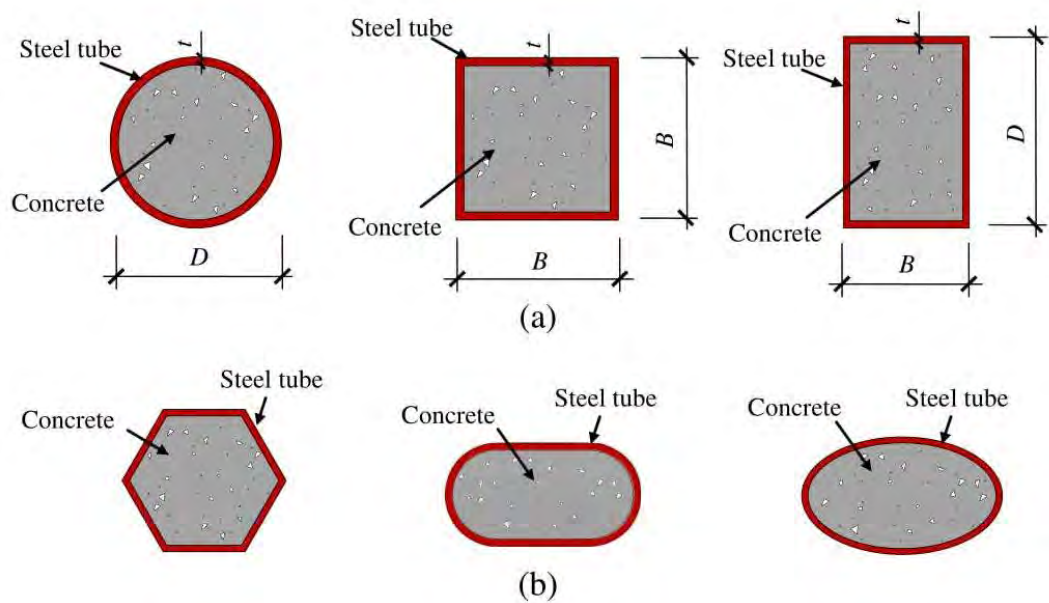
Figure 1.2 Typical concrete filled steel tubular cross sections.

It is noted that the circular cross section provides the strongest confinement to the core concrete, and the local buckling is more likely to occur in square or rectangular cross-sections. However, the concrete-filled steel tubes with SHS and RHS are still increasingly used in construction, for the reasons of being easier in beam-to-column connection design, high cross-sectional bending stiffness and for aesthetic reasons. Other cross-sectional shapes have also been used for aesthetical purposes, such as polygon, round-ended rectangular and elliptical shapes, as shown in Figure 1.2 (b).

Extensive experimental and numerical studies have been carried out by several researchers (Han et al. 2014; Sakino et al. 2004; Susantha et al. 2001; Xiamuxi and Hasegawa 2012; Zeghiche and Chaoui 2005; Zhu et al. 2010) on concentrically and eccentrically loaded CFST columns with various geometric and material properties. Most of this research work has been performed on CFST columns constructed with available standard tube shapes. However, limited research has been found on CFST

columns in built-up steel sections. Current design rules for CFST columns are specified in AISC-LRFD (2010), ACI 318R (2014), EC-4 (1994), British standard BS 5400 (2005) and Canadian Standard Association CSA (2009). CFST column is a new system for the construction industry of Bangladesh. In the upcoming version of Bangladesh National Building Code (BNBC 2016) the design guidelines for CFST columns are included which is adopted from AISC 2005 specifications. The applicability of these design provisions in the construction environment of Bangladesh needs to be explored. To this end, an attempt has been made in this study to investigate the behaviour and strength of the CFST columns constructed with built-up steel section and locally available materials.

1.2 Objectives and Scope of the Study

The objectives of this study are listed below:

a) To study the code specified design guidelines for CFST columns under concentric axial load.

b) To investigate the strength and behavior of square CFST columns under axial compression.

c) To study the effect of concrete strength, plate slenderness ratio and column overall slenderness ratio, on strength and ductility of CFST columns.

d) To compare the experimental results with the code predicted capacities for CFST columns subjected to axial compression only.

To achieve the objectives mentioned above experimental test were conducted on nine square CFST columns. The test columns had cross-sectional width of 100 mm, 125 mm and 150 mm; length of 1000 mm, 500mm and 300 mm. Specimens with different values of concrete compressive strength ($f_c^{/}$ = 20, 30 and 40 MPa), width to thickness ratio (B/t ranging from 25 to 42) and length to width ratio (L/B ranging from 3 to 10) were constructed and tested under concentric loading by using a universal testing machine (UTM). The effects of these parameters on the strength and failure behaviour of CFST columns were investigated. Finally, the experimental results were compared with the code predicted capacities.

1.3 Organization of the Thesis

This thesis is divided into seven chapters. An overview of each chapter follows.

Chapter 1 It includes the research background, objectives and the scope of the study.

Chapter 2 presents a brief review on the literature related to CFST columns and explores in relative detail research works carried out on CFST columns.

Chapter 3 contains the details of description of experimental specimens, material properties, fabrication of specimens and test module. A description of the instrumentation, end fixtures and loading condition is also included.

Chapter 4 represents all the output of this study which includes the failure mode, load-strain response, performance indexes of tested columns.

The design guidelines along with the capacity prediction equations for CFST columns is presented in **Chapter 5**. This chapter also includes the comparison of experimental and code predicted results with the three design codes ACI-318 (2014), AISC-LRFD (2010) and Euro code-4 (2005).

Finally, the summary and conclusions of the work along with the recommendations for future research have been included in **Chapter 6**.

CHAPTER 2
LITERATURE REVIEW

2.1   Introduction

Concrete Filled Steel Tube (CFST) is the composite section formed by filling concrete into a hollow steel tube. The CFST section resists applied load through the composite action of concrete and steel, this advantageous interactive behaviour between steel tubes and concrete increases the strength of CFST section. Hence, it has become popular in recent days and is being used in structures such as bridges, electricity towers, buildings etc. Extensive works carried out on CFST columns in past years have indicated that the CFST sections possess high ductility, strength and stiffness properties. These properties are considered to be important, especially for the multi-storied buildings required to be erected in earthquake-prone areas. Therefore, the behaviour of CFST sections needs to be studied. The research work on concrete-filled steel tubular structures can generally be classified as the research dealing with members, connections/joints and structural systems. The general research framework of CFST column is illustrated in Figure 2.1.
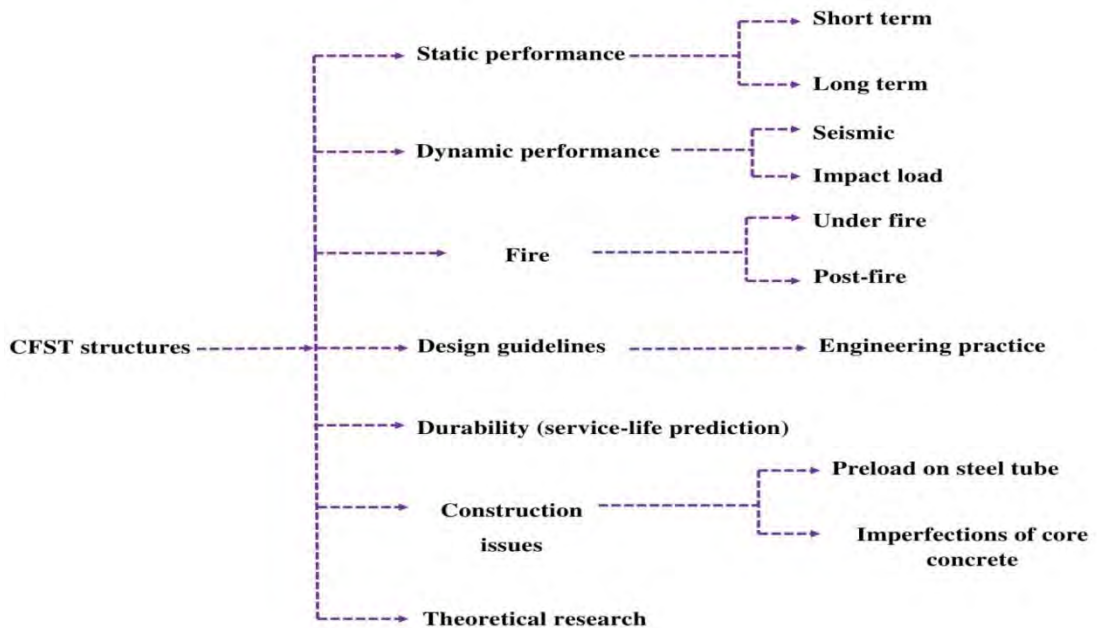
Figure 2.1 Framework of research on CFST structures.

In this chapter, a review of the research conducted on axially loaded CFST columns is presented with an emphasis on theoretical and experimental studies. A comparison of current design codes is also included. The review includes research work that has investigated the effect of concrete strength, plate slenderness ratio and column overall slenderness ratio on failure mode, load-strain response, ductility and confinement of axially loaded CFST columns. Finally, the advantages, current developments and advanced application of of CFST columns has been reviewed.

2.2   Advantages of Concrete-Filled Steel Tubular (CFST) Columns

CFST columns possess many benefits over conventional steel concrete composite columns, such as (1) the steel tube acts as formwork for the concrete core and also supports a considerable amount of construction loads during construction, which results in quick and efficient construction; (2) the compressive capacity of infilled concrete is enhanced because of the confinement effect provided by steel tubes (under bi-axial or tri-axial restraint); (3) the infilled concrete delays or eliminates local buckling of the steel tube, while the steel tube confines the infilled concrete, which prevents concrete spalling and maintains tube's stiffness after concrete cracking, so that its compressive strength can be further increased; (4) composite columns have high stiffness due to the infilled concrete.

Extensive research were carried out for studying the static properties of CFST over last several decades, the databases show that the CFST combine the benefits of steel and concrete, and the properties of CFST were favourable in terms of compression, tension, bending, shear and torsion. Han et al. (2014) provided the schematic failure modes for the CFST column under tension, bending and torsion, as shown in Figure 2.2. For the CFST member in tension (Figure 2.2 (a)), the steel tube is elongated under the tension, while there is a main crack through the whole cross-section in the concrete column. The tension performance of the CFST column is modified due to the interaction between steel tube and concrete, cracks are small and evenly distributed along the infilled concrete of CFST. Figure 2.2 (b) illustrates the failure mode of the steel tube, concrete and CFST subjected to bending moment. Cracks and crushes of the concrete are considerably altered as well as the buckling of the steel

tube wall in the CFST column. Torsion is another significant external action. Figure 2.2 (c) shows the torsional failure deformation of each member, it is apparent that the torsional deformation of the CFST is obviously decreased compared with that of the hollow steel tube. This is because the infilled concrete resists the compressive force and the steel tube resists the tensile force in the diagonal direction, a space "truss action" is formed and the local buckling is modified by the infilled concrete.
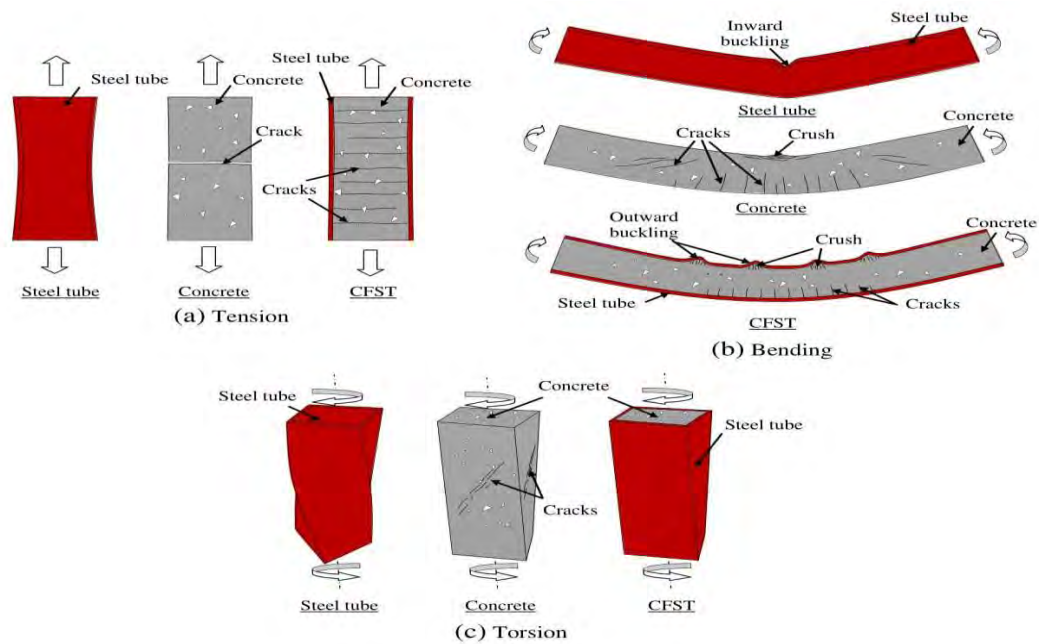
Figure 2.2 Schematic failure modes of steel tube, concrete and CFST under tension, bending and torsion.

2.3 Applications in Construction of Concrete Filled Steel Tubular (CFST) Columns

Some examples are presented here to provide some insight into how CFST column, currently, plays a significant role in civil engineering. Figure 2.3 shows the use of CFST columns in the composite steel storey system, and Figure 2.4 illustrates a subway station using CFST columns. It is well known that CFST is suitable for the supporting columns subjected to very high axial compression. Guangzhou TV Astronomical and Sightseeing Tower is the third highest in the world. It is located at the corner of Guangzhou New City Central Axes and Pearl River, as illustrated in Figure 2.5. The height of this tower is 600 m, which includes the main body (450m)

and the antenna (150 m). Twenty-four inclined concrete-filled steel circular tubular members are utilized, with a maximum tube diameter of 2000 mm and a maximum wall thickness of 50 mm (Han & Bjorhovde 2014). Figure 2.6 shows the SEG plaza in Shenzhen which is one of high-rise buildings using CFST columns.

Figure 2.3 Composite steel storey system.

Figure 2.4 CFST columns used in a subway station.

Figure 2.5 Guangzhou TV Astronomical and Sightseeing Tower.

Figure 2.6 SEG plaza in Shenzhen.

Long span is a significant feature of the CFST construction, and the hollow steel tube can be served as formwork which considerably cuts cost. Furthermore, owing to the excellent stability of the steel tubular structure, the temporary bridge becomes

unnecessary when erecting the composite arch and the construction technology for the erection can be simplified. Therefore, the application of CFST arches is in rapid development. Figure 2.7 presents the Wangcang East River Bridge, this is Chinese first steel pipe concrete arch bridge with the main span of 115 m, built in 1990. The dumbbell-shaped cross section of the main arch is also shown in Figure 2.7.

Figure 2.7 Wangcang East River Bridge.

Figure 2.8 Yajisha Bridge.

The profiles of circular steel tubes were 800 mm in diameter with 10 mm wall thickness, and the C30 concrete is used for filling hollow sections. Another CFST arch bridge is located in Guangzhou, namely, Yajisha Bridge, as shown in Figure 2.8. The main spans of the Yajisha Bridge over the south navigation channel of the Pearl River is designed as a self-anchored, half-through continuous concrete-filled steel pipe arch bridge of 3 spans of 76m+360m+76m. An innovative building method, combining vertical and horizontal awing method, has been used in erecting this bridge. Figure 2.9 shows the world's 7th longest span arch bridge, Wushan Yangtze River Bridge. This bridge is the second crossing of the 3 Gorges Dam with a span of 460 m. The main arch was constructed using the stayed cantilever method. The CFST columns have also been used in other structure, Figure 2.10 shows the Damaoshan electricity pylon completed in 2010. This carries power cables from China's Mount Damaoshan, Zhejiang Province, to the Zhoushan Islands. Comprising a tower 370 m high and 5,999 tonnes, the lattice tower carries a capacity of 600,000 kW per day. This tower is a tubular lattice with four CFST columns. The CFST column is 2000 mm in diameter, and the concrete is filled up to the height of 210 meters (Han & Bjorhovde 2014).

Figure 2.9 Wushan Yangtze River bridge.

Figure 2.10 Damaoshan electricity pylon.

2.4 Current Development of Concrete-Filled Steel Tubular (CFST) Columns

Concrete-filled steel tubular (CFST) columns have been widely used in engineering structures. In the past extensive experimental and numerical studies have been conducted in different parameters, namely: section type; section diameter; thickness of the steel tube; strengths of steel and core concrete; length of the column; load eccentricity, and so on (Schneider 1998). It is commonly accepted that CFST columns have high load bearing capacity, ductility due to the confinement effect, convenience in fabrication and construction due to the steel tube acting as permanent formwork, when compared with steel and reinforced concrete columns (Han et al. 2014). Currently, several design guidelines have been developed for the design of CFST columns in different areas, such as Eurocode 4 (2004) in Europe, DBJ/T 13-51-2010 (2010) in China, AIJ (2008) in Japan, ANSI/AISC 360-10 (2010) in U.S.A. and AS 5100.6-2004 (2004) in Australia.

To further improve structural efficiency and meet different design requirements, some recent research has focused on the development of different types of novel CFST columns. One approach is aimed at using new alloys or at changing the configuration of conventional CFST columns to improve the structural performance of composite columns. Concrete-filled double skin steel tubular (CFDST) columns consisted of two concentric steel tubes with annulus between them filled with concrete. These had almost all the same advantages as conventional CFST columns, but with lighter weight and better cyclic performance (Zhao and Grzebieta 2002; Tao et al. 2004). In the same way, stiffened CFST columns were investigated for the feasibility of thin-walled steel tubes using in CFST columns for economical purposes, where welded stiffeners were used to reduce the effect of local buckling on the thin-wall steel tubes (Tao et al. 2005). Recently, Han et al. (2010) conducted a series of tests on inclined, tapered and straight-tapered-straight CFST columns, with the aim of potentially applying these structures which may meet the architectural requirements. Furthermore, investigations on the tapered CFDST columns have been reported by Li et al. (2012), showing that this kind of innovative composite column could be used as transmission towers.

Adopting high performance steel is another approach for new development of CFST columns. Therefore, high strength steel with yield strength up to 700 MPa was used in steel tubes of CFST columns and several experimental investigations were carried out in recent years (Uy 2001; Mursi and Uy 2004). Stainless steel was another high performance steel with high strength, as well as better corrosion resistance and hardness, which has been investigated as an outer material for CFST columns by researchers for nearly a decade (Young and Ellobody 2006; Uy et al. 2011). On the other hand, since concrete also plays an important role in CFST columns, various engineers and researchers have tried to use new types of concrete other than conventional concrete to construct composite columns. For example, high strength concrete (compressive strength higher than 100 MPa) or even ultra-high strength concrete (compressive strength close to 200 MPa) could significantly increase the load-carrying capacities of CFST columns (Varma et al. 2002; Yu et al. 2008; Xiong 2012) CFST columns constructed with recycled aggregate concrete were developed

to conserve natural resources and reduce landfill requirements (Yang and Han 2006; Tam et al. 2014). The utilisation of lightweight aggregate concrete in CFST columns was proposed to reduce the structural weight significantly (Fu et al. 2011a; Fu et al. 2011b).

2.5   Research on Axially Loaded Concrete Filled Steel Tube Columns

The behaviour of CFST columns has been the subject of numerous experimental and theoretical studies since Kloppel and Godar (1957). Tests have been performed on short and slender columns under a variety of axial and eccentric load conditions. Detailed experimental studies into the enhanced strength and ductility of short columns have been published. Accompanying such investigations a multitude of design models derived empirically or theoretically. Such research has lead to the implementation of CFST design provisions in several International design standards. Due to variations analytical procedures, design philosophy or empirical data-bases used, significant discrepancies exist with respect to quantifying the ultimate capacity of the composite section. This non-uniformity has emphasized the importance of further research required into the behavior of CFST columns. Table 2.1 shows the summary of past literatures on axially loaded concrete-filled steel tubular columns. Findings of these experimental studies are presented below:

Table 2.1 Experimental studies on axially loaded CFST column test.

Reference	Experimental Synopsis	Number of Tests	Main Parameters
Kloppel and Gorder 1957	Concentrically loaded CFST and HST	104 tests	
Knowles and Park 1969	Concentric and eccentric loading of columns	28 CFST (18 concentric, 10 eccentric) and 30 HST (20 concentric, 10 eccentric)	• Type of tubing • D/t • L/D • e
Kitaba et al. 1987	Short CFST columns subjected to axial compression.	14 CFST	

Zhong and Miao 1988	Short CFST columns subjected to axial compression.	11 CFST	• L/D ratio • Steel ratio • End conditions
Luksa and Nesterovich 1991	Large diameter CFST under axial compression.	30 CFST and 10 HST	• D • t
Masuo et al. 1991	Concentric testing of lightweight concrete CFST	26 CFST	• D/t • Slenderness ratio
Sakino and Hayashi 1991	Concentrically loaded stub columns.	7 CFST and 5 HST	• D/t • $f_c^{/}$
Bergmann 1994	Concentrically loaded circular and square CFST with different load introduction.	16 CFST	• Section shape and size • Load introduction • Length
Tsuda et al. 1996	Concentrically and eccentrically axially slender CFST	48 CFST (24 circular, 24 square) and 12 HST	• Eccentricity • Buckling length-section depth ratio (kL/D).
Oshea and Bridge 1997	Concentric loading of square box HST and square box CFST filled with unbonded and bonded concrete.	17 CFST (concentric) and 12 HST (concentric)	• CFT vs. HT • L/D, D/t
Shakir Khalil et al. 1997	Concentric & eccentric loading of full-scale rectangular CFST	11 CFST (concentric) and 11 CFST (eccentric)	• L/D • λ • e_x • e_y

Schneider 1998	Monotonic axial loading of circular, square and rectangular CFST.	14 CFST	• D/t • Shape
Zhang and Zou 2000	Monotonic axial loading of CFST	36 CFST	• D/t • f_y
Han and yan 2001	Monotonic loading of square CFST	8 CFST (concentric) and 21 CFST (eccentric)	• f_c' • D/t • Magnitude of eccentricity • Slenderness
Johansson and Gylltoft 2002	Short circular CFST columns subjected to axial compression with different methods of application.	9 CFST and 4 HST	• Load application • HST/CFST
Giakoumelis and Lam 2004	Short circular CFST columns subjected to axial compression	13 CFST and 2 HST	• f_c' • bond
Guo et al. 2007	Monotonic behavior of steel only loaded unbonded square CFST	12 CFST and 12 HST	• D/t • CFT/HT
Uy 2008	Concentric axial load on CFT Column.	8 CFST	
Uy 2011	Eccentrically and concentrically loaded stainless steel CFST and HST.	33 HST (2 eccentric, 31 concentric) and 84 CFST (all concentric)	• D/t • f_c' • e
Mahgub et al. 2016	Test on self compacting elliptical CFST column.	8 CFST and 2 HST	• f_c' • L/D

Knowles and Park (1969)

This paper investigated axially loaded CFTs and hollow tubes over a wide range of slenderness ratios, with particular attention paid to the effect of the slenderness ratio on the lateral pressure exerted by the tube on the concrete. The authors also looked at the effect of loading the materials together and individually (i.e., load the concrete and not the steel and vice versa). They examined concentrically loaded columns theoretically by the tangent modulus approach and they constructed a straight line interaction formula to estimate the behavior of eccentrically loaded CFTs.

All of the hollow tubes tested under axial loads failed by inelastic flexural buckling; no local buckling was observed before the ultimate load was reached. Since local buckling is often sudden and catastrophic, the authors suggested that the ratio of the wall thickness to the diameter of the tube should be limited, although no specific values were given. The concrete-filled tubes failed in the same manner as the hollow tubes, with the region of plasticity always located at mid height. It was noted that the square tube columns with small slenderness ratios did not gain additional strength due to confinement. Although it has been shown by other investigators that square tubes provide less confinement than circular tubes, square ties in reinforced concrete have produced good confinement results. The authors stated that the issue of square tube confinement has yet to be resolved.

Zhong and Miao (1988)

A standard test for short CFTs was developed to provide a basis to correlate results from different sources and to provide stress-strain input for design formulations. In lieu of experimental results, the authors also developed an analytical method to determine key points on the stress-strain curve which could be used for in computing the ultimate design strength of the CFTs.

The main goal of the standard test was to accurately obtain the longitudinal stress-strain relationships in the steel and the concrete for use in a design method. This required a test on short columns that would not fail by buckling. Columns having an L/D ratio ranging from 2.0 to 5.0 were selected for study. From their tests, the

authors concluded that a standard test should use an L/D of 3.0 to 3.5. Tubes with a ratio of 3.5 showed no unloading, remained essentially straight throughout the test, and had constant strain through the cross-section. This was not the case, however, for specimens with L/D greater than 4.0. The lower limit of 3.0 was to avoid significant end effects. They also recommended using plate hinges for end supports.

Luksa and Nesterovich (1991)

The behavior of large diameter CFT members under axial compression was investigated and the authors noted some of the failure peculiarities of the specimens. The discussion of the large diameter failures was quite detailed.

Ten sets of specimens were tested, 3 CFT and 1 HT in each set. The main parameter of interest was the diameter of the tube. Each set had a different diameter varying from 6.25 in. to 40.2 in. The steel tubes were welded and filled with heavy concrete of unspecified weight and the L/D ratio was 3. Two types of failure were recognized in the study. Small diameter tubes were characterized by local buckling around the end of the specimen accompanied by crushing of the concrete in this zone. The large diameter specimens failed in shear. The failure began at 90% of the ultimate load by the formation of buckles along the cylinder's diagonal. The failure lines on the tube shifted before failure, and an oblique crack formed in the concrete at about a 25 to 35 degree angle to the vertical. Just before the shift occurred, the radial compressive stresses in the concrete reached their maximum value. The concrete shifted and the load between this point and failure increased very little as the steel buckled. The authors alluded to analytical results from an earlier paper and compared their experimental results to these values.

Masuo et al. (1991)

The buckling behavior of CFT columns was studied both experimentally and analytically, using both lightweight and normal weight concrete subjected to concentric axial load. Ultimate loads were discussed with regard to three parameters: concrete weight, size of the steel tube, and effective column length.

The initial deflection at mid-height for columns in this range of slenderness ratios was computed as the deflection of the column before the test divided by the effective length. In the tests, an initial deflection of L/4000 or L/8000 was used, the higher number for more slender columns. The authors found that both weights of concrete with slenderness factors around 0.3 were definitely affected by confinement, the normal weight concrete showing a somewhat larger effect. The load-deflection relations were also significantly affected by the confining effect in this range of slenderness factors. Several detailed graphs elucidate this point. Varying the D/t ratio from 30-40 and holding the other test parameters constant did not seem to affect the squash load. Finally, the ultimate loads of the CFTs for both weights at a slenderness factor of 0.6 were somewhat larger than the European column curve.

Sakino and Hayashi (1991)

The axial load-longitudinal strain behavior of CFT stub columns with circular cross-sections was analyzed and compared to experimental tests. The effect of different D/t ratios and different concrete strengths was investigated. Studies were also conducted regarding the ratio of hoop strains to longitudinal strains in the steel tube. The main objective was to estimate the effects of both strain hardening of the steel tube and the triaxial confinement of the concrete core. The introduction to the paper presented a concise summary of the nature of stresses in the components of a CFT as the load increases.

The analytical and experimental results agreed quite well except for the specimens containing 'high-strength' concrete (6.5 ksi) and having a large D/t ratio. To predict the behavior of high-strength concrete in large deformation regions, the effect of work softening must be considered. The observed maximum axial load capacities were 1.12-1.25 times the analytical capacity, with the effect of strain hardening ignored. The theoretical and experimental results showed that the ratio of the hoop strain to the longitudinal strain became greater than 0.5 under large strains, indicating the concrete dilates in the plastic region. The hoop strain to longitudinal strain ratio increased with an increase in the D/t ratio and increased slightly with an increase in the concrete strength. However, the theoretical values were less than the

experimental, prompting the authors to suggest the need for an alternative to the assumed associated flow rule.

Bergmann (1994)

Sixteen tests were performed to investigate the behavior of CFT columns with high strength concrete under various methods of load introduction. The specimens that were loaded only on a small portion of the concrete experienced local failures at the point of load application and exhibited lower strength than the other specimen. The strength of three of the four specimens with the larger circular cross-section exceeded the capacity of the testing machine and only a lower bound of load was determined. The load deformation curves of the remaining specimens exhibited similar traits. Most notably, upon reaching ultimate load, the strength decreased suddenly, followed by a relatively constant strength.

Tsuda et al. (1996)

An experimental study conducted on circular and square CFT beam-columns was presented in two companion papers (see also Matsui et al., 1995). The behavior of CFT specimens was examined under axial loading and combined axial and flexural loading. Columns having a wide range of L/D ratios were tested. The experimental results were compared with AIJ (1987, 1990) and CIDECT (1994) design code provisions.

It was observed that the specimens having a higher magnitude of eccentricity exhibited lower axial strength and larger mid-height deflection. The effect of eccentricity decreased for high L/D ratios. The columns with L/D ratios less than 18 achieved the plastic moment capacity. The circular specimens in this range even exhibited larger capacities due to the confinement effect. For square specimens, the confinement effect was not observed. The capacities of the columns having L/D ratios above 18 could not attain the plastic capacity due instability effects.

Shakir Khalil et al. (1997)

Stub columns of rectangular CFTs were first tested to determine the squash load of CFT members. Column CFT specimens were then tested monotically in a horizontal position. Pin-ended support conditions were simulated by the test setup. The L/D ratios were ranging from 21 to 49. For major and minor axis bending, the D/t ratio of the specimens was 30 and 20, respectively. The applied eccentricities did not exceed one half the diameter of the column. The yield strength of steel was varying from 47.0 ksi to 53.3 ksi. The compressive strength of concrete ranged between 5.3 ksi and 6.0 ksi. The stub columns exhibited 16 to 30% higher strength than their nominal axial load capacity calculated according to BS5400 (1979). Their strength was observed to decrease with an increase in length due to local buckling. The local buckling generally took place at the longer side of the tubes. The concrete was investigated after testing. It was crushed but kept its integrity, thus facilitating the achievement of the large strengths in the stub columns. In addition, the CFT columns were found to have an increase in strength of 25-37% over similar hollow tubes. Except for one case, the failure load decreased with an increase in end eccentricity. This was because that specimen experienced pure bending response about the major axis. The authors noted that the behavior of columns subjected to small eccentricities about the major axis was especially sensitive to any imperfections, most notably, out-of-straightness.

Zhang and Zou (2000)

An experimental and an analytical study on square CFT columns were presented. The steel tube response was isolated from the overall behavior of the specimens and the response of the concrete and steel were examined separately. Formulations were proposed for the confined concrete strength, the confined concrete strain, and the longitudinal stress in the steel tube.

Thirty-six CFT columns were tested under monotonically applied axial loading. The D/t ratio of the specimens ranged between 20 and 50. The measured compressive strength of concrete was 5.87 ksi and the yield strength of the steel ranged from 41.28 ksi to 58.51 ksi. The L/D ratio varied between 4 and 5. From the experimental

results, it was found that the confinement effect increased the concrete strength and ductility. They also determined that the longitudinal stress in the steel tube was always less than the yield stress due to the biaxial stress condition. Confinement was found to be larger when the D/t ratio was smaller.

Han and yan (2001)

A series of monotonic tests were conducted on square CFTs including stub-columns, columns, and beam-columns. In addition, the authors presented analytical models to estimate the capacity and load-deformation response of the specimens.The objective of the experiments was to investigate the strength and failure patterns of CFTs. Two sets of experiments were conducted. In the first set, twenty stub-columns were tested. Eight columns and twenty-one beam-columns were tested in the second set. The authors defined a confinement factor to account for the composite action between steel and concrete. This factor was used as a parameter in each set of experiments, with a range of values varying from 1.08 to 5.64. Other parameters included concrete strength, D/t ratio, eccentricity, and slenderness. The average measured yield strength of steel was 47.14 ksi and the measured cubic concrete strength ranged between 2.35 ksi and 7.15 ksi. The D/t ratio varied from 20.5 to 36.5.

Johansson and Gylltoft (2002)

The behavior of circular CFT stub columns subjected to monotonic compression was analyzed and compared to three-dimensional nonlinear finite element models. The primary focus was the effect load placement on the structural behavior of CFTs. The distribution of the load between the steel tube and concrete core at the mid-height of the column was illustrated for the different loading configurations. While the peak axial capacity of the CFTs with their entire cross-section loaded and the CFTs with only their concrete loaded is nearly the same, the distribution of the loads is different. When only the concrete is loaded, the steel tube carries at most 30% of the load, while, when the entire cross-section is loaded, the steel tube carries about 40% of the load. When only the steel was loaded, no redistribution of the force was noted and the steel carried 100% of the load. Examination of the load distribution also gave insight to the difference in initial stiffness between CFTs loaded on the concrete only

and the CFTs loaded on the entire cross-section. When loaded on the entire cross-section, the load is distributed by bearing from the start. When loaded on the concrete only, stress in the steel is developed through friction at the interface, a more gradual process.

Giakoumelis and Lam (2004)

This paper presents the results of tests on circular CFT columns. The effect of bond between the steel tube and concrete core for a range of concrete strengths was examined. The experimental results were compared to European, American, and Australian design codes.

The main test parameters were concrete strength, steel tube thickness, and bond between the concrete core and steel tube (greased or non-greased). The diameter of the steel tube and length of the column remained constant for all tests, with an L/D ratio of 2.6. Three different concrete strengths were used (4.3 ksi, 8.6 ksi, and 14.3 ksi). The nominal yield strength of the steel was 50 ksi, the measured value was obtained from compressive tests on hollow tubes. The columns were capped on both ends to distribute the load uniformly over the steel and concrete.

It was observed that for high strength columns, the peak load was obtained with small displacement, whereas the for normal strength columns the peak load was obtained with large displacements. It was further observed that the difference between the greased and non-greased specimens varied with the compressive strength of the concrete. For normal strength concrete the load displacement curves for the two were nearly identical. For medium strength concrete, at ultimate load, the greased and non-greased achieved the same capacity, but the elastic capacity was higher for the non-greased specimen. For high-strength concrete a significant variation between greased and non-greased specimens was noted.

The experimental results were compared to Eurocode 4, ACI 318-95 and Australian Standards AS3600 & AS4100. While all methods provided conservative results, the Eurocode 4 method provided the most accurate results. The authors noted that neither

the ACI nor the Australian Standards method take into consideration the concrete confinement. Thus a constant coefficient was proposed to account for the confining effects.

Guo et al. (2007)

The results of steel only loaded square CFT columns are presented along with a corresponding numerical model. The results from additional numerical studies are used to formulate design recommendations applicable to RCFT columns with a wide range of D/t ratios.

Twelve square CFT and twelve square HT short columns tests were performed. The CFT columns were loaded on the steel only, 0.59 in gaps without concrete were left at each end of the columns, and the steel was greased before placing the concrete to inhibit bond. All of the tubes were fabricated from two L shaped mild steel plates welded at their tips to form a square cross-section. The yield strength of the steel was 40.6 ksi. The thickness of the steel plate was constant, 0.063 in., while the depth was varied from 3.14 in. to 7.88 in to achieve D/t ratios between 50 and 125. The length was varied to keep L/D ratio equal to 3.0. End plates with a thickness of 0.31 in were welded to the ends of the CFTs. Stiffeners were welded to both ends of each specimen in accordance with Chinese design. The concrete used had a compressive strength of 5.6 ksi.

The initial stiffness was nearly identical between the CFTs and HTs, indicating that the concrete was, indeed, not carrying any load. The presence of the concrete prevented the occurrence of inward local buckles and the wavelengths of the local buckles were considerably smaller than those occurring in the HTs.

Uy (2008)

This paper aims to investigate the stability and ductility characteristics of concrete filled columns using high performance steel (HPS). Previous research in HPS and

current applications of HPS are discussed at length. Eight columns were tested under compression as two hollow high strength steel and two hollow stainless steel box sections were compared to two concrete filled high strength and stainless steel box sections.

The high strength steel columns considered were constructed with a box section of 4.3 x 4.3 in. with a 0.197 in. nominal plate thickness. A nominal yield stress of 65 ksi was chosen. The hollow sections exhibited quite ductile behavior. The concrete filled sections reached a peak load and gradually experienced a load reduction; the author attributes this to internal concrete crushing. The paper suggests that confinement is less likely to take place for high strength steel sections because the strains at which yields are often achieved are often in the vicinity of the crushing strains of most normal strength concrete.The stainless steel columns had a nominal dimension of 3.94 x 3.94 in. cross section with 0.197 in. nominal wall thickness. The tensile coupon tests revealed a mean 0.2% proof stress of this material to be about 32 ksi and the mean ultimate stress to be about 61 ksi. The hollow section columns achieved a maximum load just larger than 180000 lbs., at which point loads began to stabilize. Results for the concrete filled steel sections revealed that the presence of the concrete infill allowed local buckling to be considerably delayed and a gradual increase in the steel allowed. Furthermore, the steel section appeared to significantly confine the concrete in these sections.

Uy et al. (2011)

This paper discusses axial compression tests performed on concrete filled steel tubes, as well as hollow steel sections. A combination of circular, square, and rectangular columns were tested. The specimens were divided into four groups; group 1 was composed of 72 short columns under axial loading, group 2 was 9 short columns, group 3 was 12 short beams-columns under axial compression and bending, and group 4 was 24 columns under axial loading. Group 2 investigates how a different loading method may affect the results, and group 4 investigates slender columns. Group 3 which was under combined loading, displayed very ductile characteristics, and both the strength and stability were significantly increased. For the short

columns, short knife edges were placed on the end plates, and grooves were added to the plates to apply moments. For group 4, two hinges were added to both ends of the column to simulate pin-ended supports. Two strain gauges were added to both sides of each short column for a total of six gauges per column. Deflection for the short specimens was measured at mid height due to limited space. Longitudinal and transverse strains were measured using strain gauges with a length of 3mm. Both circular and square CFST columns displayed local outward folding failure, and thicker sections displayed local buckling at mid-span height. With the square hollow sections, local buckling occurred in convex and concave surfaces. The columns with a larger D/t ratio displayed less ductile characteristic than a column with a smaller D/t ratio. The specimens using stainless steel over carbon steel displayed more ductile behavior and a greater residual strength. The specimens using high-strength concrete had a compressive strength of two times the normal strength of concrete.

Mahgub et al. (2017)

This paper presents an experimental study into the axial compressive behaviour of self compacting concrete filled elliptical steel tube columns. In total, ten specimens, including two empty columns, with various lengths, section sizes and concrete strengths were tested to failure. The experimental results indicated that the failure modes of the self-compacting concrete filled elliptical steel tube columns with large slenderness ratio were dominated by global buckling. Furthermore, the composite columns possessed higher critical axial compressive capacities compared with their hollow section companions due to the composite interaction. However, due to the large slenderness ratio of the test specimens, the change of compressive strength of concrete core did not show significant effect on the critical axial compressive capacity of concrete filled columns although the axial compressive capacity increased with the concrete grade increase. The comparison between the axial compressive load capacities obtained from experimental study and prediction using simple methods provided in Eurocode 4 for concrete filled steel circular tube columns showed a reasonable agreement. The experimental results, analysis and comparison presented in this paper clearly support the application of self-compacting concrete filled elliptical steel tube columns in construction engineering practice.

Ibanez et al. (2018)

An experimental investigation of 12 concrete-filled steel tubular (CFST) stub columns subjected to concentric loads was carried out. In this program, different cross-sectional shapes were considered: circular, square and rectangular. In order to study the effect of the concrete infill strength in the ultimate capacity of the columns, two types of concrete infill were employed: normal and high strength concrete of grades C30 and C90 respectively. The experimental ultimate loads of the specimens were compared with the corresponding failure loads given by the codes. In this case, comparison showed that Eurocode 4 and the Chinese and Australian standards overestimate the failure load of the specimens, particularly for square and rectangular CFST columns. The American code tends to be more conservative in its predictions for circular columns.

2.6   Conclusions

Considerable progress over the last 40 years has been made in the investigation of CFST columns. Fundamental knowledge on composite construction systems has already been obtained by the researcher. However, intensive research is required, on the applicability of the design provisions in the construction environment of Bangladesh. While much of the current available research draws similar conclusions on the behaviour of CFST columns, there are a number of conflicting views being documented. In investigating CFST columns under compression, previous studies have mainly focused on their compressive strength. Very little attention has been paid to their compressive stiffness and deformation capacity. For structural analysis, compressive stiffness of a member affects the internal force distribution; therefore accurate values should be provided. Meanwhile, designers nowadays are paying more attention to extreme loading, such as seismicity, impact and fire; and other abnormal events. Accordingly, the issue of ductility or deformation capacity is of considerable interests to the designers. Therefore, this experimental study is mainly focused on the failure mode, load-strain response and ductility of the square CFST column.

CHAPTER 3
EXPERIMENTAL PROGRAM

3.1 General

An experimental investigation, to determine the complete failure modes and load-deflection behavior of CFST columns is presented in this study. The main variables considered in the test program were concrete compressive strength, cross-sectional dimensions, and column overall length. The loads were applied concentrically on top of the plate of CFST columns. The failure modes, peak load, peak strain and experimental load-deflection behaviour of the specimens were examined for concentric loading. The composite column specimens were tested in the Solid Mechanics Laboratory of Bangladesh University of Engineering and Technology (BUET), Dhaka, Bangladesh during the month of June in 2018. The description of the test specimens, test setup, loading conditions are presented in the following sections. Figure 3.1 shows the pictorial view of experimental investigation.
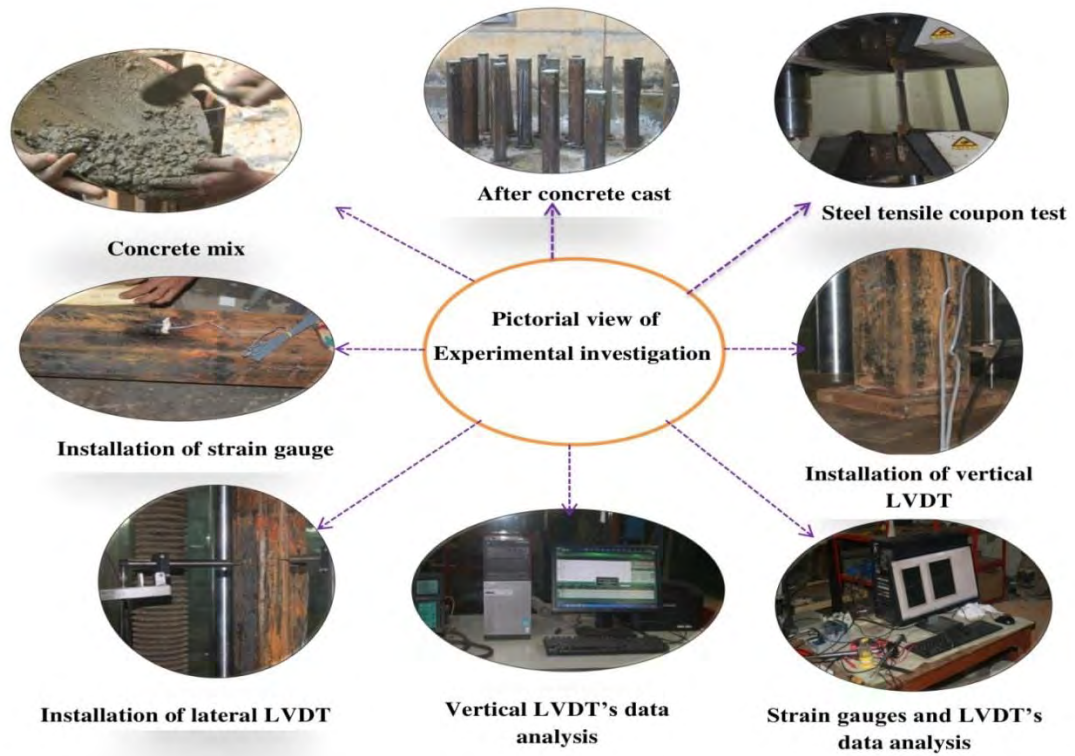
Figure 3.1 Pictorial view of experimental investigation.

3.2 Description of Test Specimens

Total nine CFST columns with square cross section were tested under concentric loading. Figure 3.2 shows the cross-section and elevations of a typical square CFST column. The geometric parameters illustrated in the plan view Figure 3.2 (b) are the width (B) and tube thickness (t) of CFST column. The column length, L is illustrated in the elevation view in Figure 3.2 (a). The tested columns had a cross sectional width (B): 100, 125 and 150 mm; length (L): 1000, 500 and 300 mm; tube thickness (t): 3, 4 and 5mm; concrete compressive strengths (f_c'): 27, 35 and 44 MPa. The geometric properties of the test specimens are given in Tables 3.1.

(b) Square cross-section of column

(a) Elevation of composite column C1
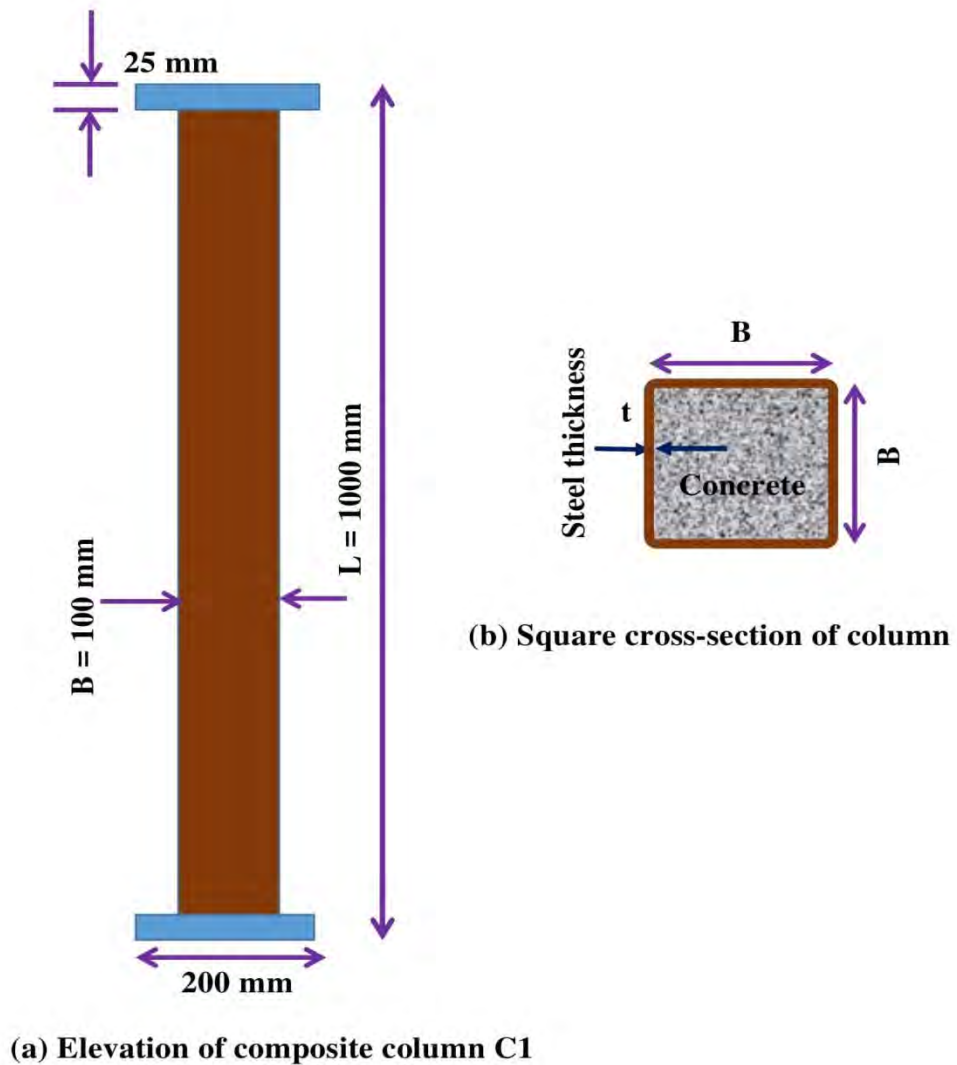
Figure 3.2 Geometry of CFST columns.

Table 3.1 Geometric properties of test specimens

Specimen design	Cross-sectional size	Width to thickness ratio	Length to width ratio	Concrete compressive strength	Yield stress
	B x t x L	B/t	L/B	$f_c^{/}$	f_y
	(mm x mm x mm)			(MPa)	(MPa)
C1	100 x 4 x 1000	25	10	27	350
C2	100 x 4 x 1000	25	10	35	350
C3	100 x 4 x 1000	25	10	44	350
C4	125 x 3 x 1000	42	8	35	350
C5	125 x 4 x 1000	31	8	35	350
C6	125 x 5 x 1000	25	8	35	350
C7	100 x 4 x 500	25	5	35	350
C8	100 x 4 x 300	25	3	35	350
C9	150 x 4 x 1000	37.5	6.6	35	350

3.3   Explanation of Test Parameters

The parameters considered in the test were: concrete compressive strength ($f_c^{/}$): 27 Mpa to 44 Mpa; width to thickness ratio (B/t): 25 to 42; length to width ratio (L/B): 3 to 10. Specimens C1, C2 and C3 were constructed with concrete compressive strength ($f_c^{/}$): 27, 35 and 44 MPa respectively. The parameters varied between these columns were concrete compressive strength. The columns C4, C5 and C6 were designed to have width to thickness ratio (B/t): 42, 31 and 25 respectively. These three specimens were designed to examine the cross-sectional effect on the behavior of CFST column. Effect of Column overall slenderness was examined with the specimen of C2, C7 and C8 which had length to width ratio (L/B): 10, 5 and 3 respectively.

3.4   Test Column Fabrication

There are mainly two parts in CFST columns i.e. steel and concrete. The steel part consists of steel tube , top and bottom plates. The structural steel tubes were fabricated by McDonalds Steel Building Products Ltd, Dhaka, Bangladesh. concrete was poured in to the steel tube for the construction of CFST columns.

3.4.1 Steel section fabrication

All the steel tubes were fabricated by joining two channels through continuous welding. The thickness of the tube was measured by a screw-gauge at four places and the mean value was taken. Using a vernier caliper, the wide of the tube was measured. All the steel tubes were machined and welded to 20mm thick steel bottom plate. End plate was welded to each of specimen for uniform distribution of the applied load.

3.4.2 Mixing, placing and curing of concrete

Cement, fine aggregate and coarse aggregate were weighed and batched as per the required quantity. An electrically operated concrete mixer was used for mixing the concrete. The materials are mixed in a mechanical mixer of revolving drum type. The main purpose of mixing is to produce an intimate mixture of cement, water, fine and coarse aggregate of uniform consistency throughout each batch. To cast all the CFST columns, three types of concrete mixes were used: M20, M30 and M40. The mix designs are presented in Table 3.2.

Table 3.2 Mix designs for plain concrete

| Mix design | Cement (OPC) | Coarse aggregate | | Fine aggregate | Water |
		¾ inch black stone	½ inch black stone chips		
	(Kg/m^3)	(Kg/m^3)	(Kg/m^3)	(Kg/m^3)	(Kg/m^3)
M20	355	711	305	799	185
M30	385	719	308	732.5	181
M40	435	699	299	712	183

For composite columns the empty steel tube was kept ready for placing of concrete. The tubes were filled in a vertical position. Concrete was poured into the steel tube from top. The tube was placed on a smooth surface before concreting. The concrete was compacted by means of a needle vibrator. The compaction by tamping rod is used for adopting high water cement ratio to enable the concrete to flow readily around the tube. The compaction by needle vibrator was used for all mixes. Such compaction prevents honeycombing, ensures more impermeable and dense concrete,

better bond between concrete and steel tube. After filling the tube the concrete was finished smooth at the top. The specimens cured with water after the day of casting for 28 days. To avoid surface water evaporation jute and polyethylene sheets were used. Figure 3.3 shows the mixing, placing and compacting of concrete.

(a) Mechanical mixture

(b) Fresh Concrete

(c) Hollow steel tube

(d) Concrete placement

(e) Compaction

(d) Constructed CFST columns

Figure 3.3 Mixing, placing and compacting of concrete.

3.5   Material Properties

The CFST columns consist of steel tube and concrete. To determine the stress-strain characteristics of the steel plate in tension, tensile coupons were conducted on steel plates. Concrete cylinders were cast and tested to ascertain the characteristic compressive strength of the concrete. In total eighteen cylinders were tested for the three types of concrete strength used in this study.

3.5.1   Steel

The mechanical properties of steel materials were measured by tensile coupon test according to ASTM D638-02a (2003). Three steel plate samples were tested to determine the material properties of steel. Typical stress-strain diagram and the dimensions of each coupon are shown in Figure 3.4. The tension tests on plates were conducted in the universal testing machine (UTM), with a tensile capacity of 2000 kN, in the Structural Mechanics laboratory of BUET. Load measurements were taken using the internal load cell of the UTM. The results of the steel-plate tension tests are given in Table 3.3.

Table 3.3 Tensile properties of structural steel tube plate.

Specimen no.	Yield Stress (f_y)	Ave. (f_y)	Ultimate Stress (f_u)	Ave. (f_u)	Elastic modulus (E_s)	Yield strain (ε_y)	Ave. (ε_y)	Ultimate strain (ε_u)
	(MPa)	(MPa)	(MPa)	(MPa)	(MPa)	($\mu\varepsilon$)	($\mu\varepsilon$)	($\mu\varepsilon$)
1	352		423		200000	2150		27167
2	350	350	428	428	200000	2148	2148	25167
3	348		433		200000	2146		33159
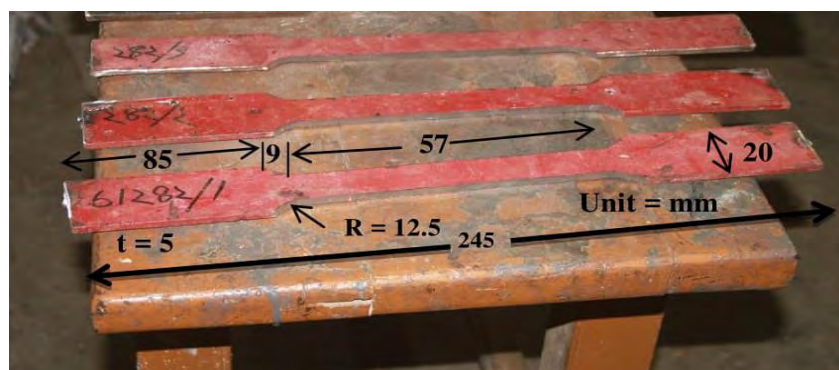
(a) The dimensions of coupo
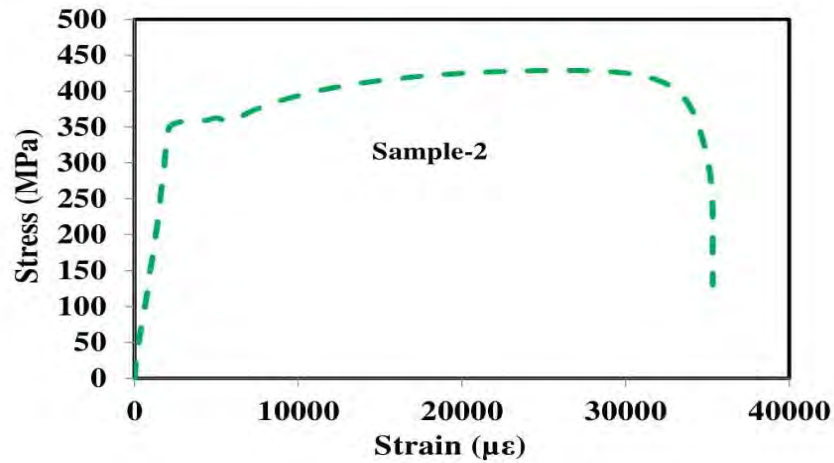
(b) Typical stress-strain diagram of tensile coupon test

Figure 3.4 Tensile coupon test of steel tube.

3.5.2 Concrete

A total of three mixes were required to batch the nine CFST columns. Three different strength of concrete (20, 30 and 40 MPa) were cast for constructing these columns. In order to determine the material properties, six concrete cylinders with (4inch*8inch) were cast from each mix. The designation of the individual cylinder for three different strength of concrete is shown in Table 3.4. Twenty four hours after casting, cylinders were removed from molds and kept in the lime water. Nine concrete cylinders (three from each mix) were brought out from the lime water after 28 days to determine the compressive strength of concrete and the other nine cylinders were tested during the day of column testing.

Table 3.4 Designation of concrete cylinder for different strength

Concrete strength	Cylinder designation
20 MPa Column symbol (C1)	20CY1, 20CY2, 20CY3, 20CY4, 20CY5, 20CY6
30 MPa Column symbol (C2, C4, C5, C6, C7, C8 & C9)	30CY1, 30CY2, 30CY3, 30CY4, 30CY5, 30CY6
40 MPa Column symbol C3	40CY1, 40CY2, 40CY3, 40CY4, 40CY5, 40CY6

All cylinders were capped with a high strength capping compound prior to testing to ensure uniform bearing in the testing machine. Cylinders were tested in the concrete Materials Laboratory at BUET. The compressive strength of all twelve cylinders is given in Table 3.5. Average compressive strength of these cylinders (M20, M30 and M40) after 28 days were found to be 27, 35 and 44 MPa. Remaining cylinders were tested at the same day of testing CFST columns. Average compressive strength of those cylinders were slightly greater than 28 days compressive strength. This variation was due to the reason that concrete gains strength with time.

Table 3.5 Concrete cylinder strength

Concrete Strength	Column symbol	Designation of cylinders		Strength		Strength increase (28 day to test day)	
		28 day	Test day (40 day)	28 day (MPa)	Test day (MPa)	(MPa)	(%)
20 MPa	C1	20CY1	20CY4	26.5	27.4	+0.9	3.4
		20CY2	20CY5	25.9	26.7	+0.8	3.0
		20CY3	20CY6	25.6	26.9	+1.3	5.0
Mean				26	27	1.0	3.8
30 MPa	C2 C4 C5 C6 C7 C8 C9	30CY1 30CY2 30CY3	30CY4 30CY5 30CY6	34.6 33.5 33.9	35.8 34.6 34.6	+1.2 +1.1 +0.7	3.5 3.3 4.8
Mean				33	35	1.0	3.9
40 MPa	C3	40CY4	40CY4	41.9	44.4	+2.5	5.9
		40CY5	40CY5	42.5	43.7	+1.2	2.8
		40CY6	40CY6	41.6	43.9	+2.3	5.5
Mean				42	44	2.0	4.7

3.6 Test Setup and Data Acquisition System

All the tests were performed using a 2000kN loading capacity universal testing machine (UTM). The columns were aligned vertically and centred in the UTM to provide uniform bearing. The experimental setup of the tested specimens is shown in Figure 3.5. Four strain gauges were used on two faces of steel tube to measure the longitudinal and transverse strains of the tube, where linear variable differential transducers were used to measure out of plane deflection in vertical and lateral

direction. Displacement control loading at a rate of 0.5 mm/min was used throughout the loading of the test specimens. The data acquisition system used two PC running Horizon data acquisition software and Labview software. The digital reading of UTM machine were collected from Horizon data acquisition software and the readings of LVDT and strain gauges were collected from Labview software.
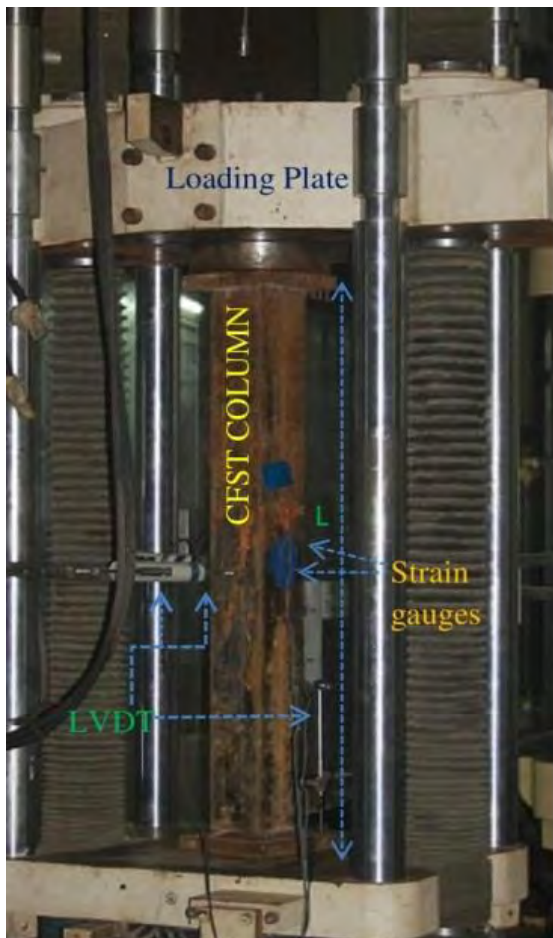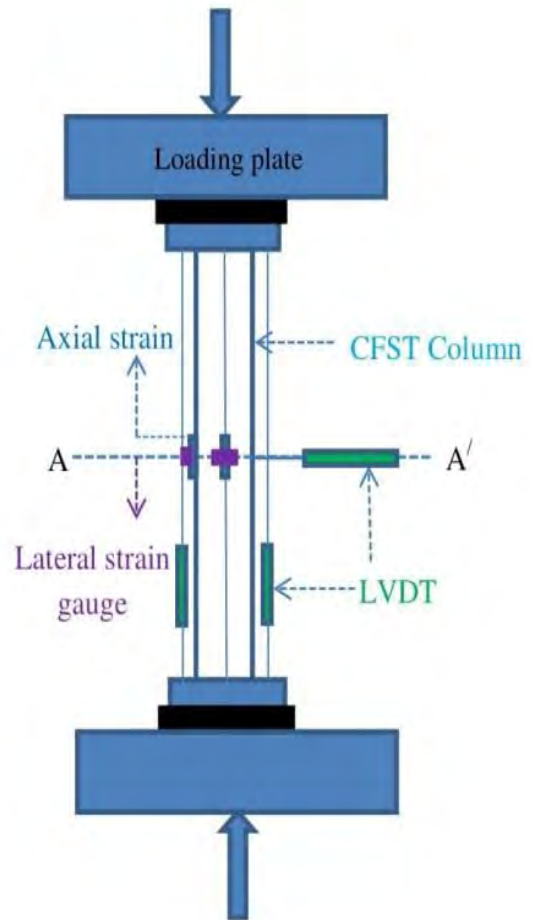
(a)   (b)

CHAPTER 4
RESULTS AND DISCUSSIONS

4.1   General

In this study, an experimental program has been designed to investigate the behavior and failure mode of concrete filled steel tubular column. Total nine CFST columns with square cross section were tested under concentric loading. The parameters considered in the test were: concrete compressive strength**,** plate slenderness ratio and global slenderness ratio. Axial load, axial strain and failure modes of the columns were obtained from the experimental test. The performance indexes such as ductility index, concrete contribution ratio, steel contribution ratio and strength reduction factor were also determined to observe the performance and cost effective design of CFST column. All the results obtained from the experimental investigation were organized and presented to highlight the individual effect of each parameter. In the following sections, the significant observations from the experimental study have been reported along with the relevant tables and figures.

4.2   Failure Modes

Generally global slenderness ratio (L/D), plate slenderness ratio (B/t) and concrete infill have a significant effect on the failure mode of the CFST column. Figure 4.1 illustrates the typical failure modes of the CFST column.

During the loading process, there is no obvious deformation at the beginning of the loading for all the columns. When the load was applied near the ultimate load, cracking sounds were audible, and then buckling on the columns appeared. The configurations of the columns after the testing are shown in Table 4.1 and Figure 4.2. Close observation of the tested columns leads to the following:

   i.   Only outward local buckling was observed for square CFST columns due to the presence of the core concrete. But for square hollow tubes, both outward and inward local buckling appears along the steel plates.

   ii.   For columns (C1, C2 and C3) with higher L/B ratio, failure was initiated by global buckling followed by crushing of concrete. Because the columns with

higher slenderness ratio had greater flexibility which resulted in larger mid-height lateral displacement.

iii. Columns (C4, C5, C6 and C9) with higher B/t ratio failed by outward local buckling followed by crushing of concrete. Outward local buckling of the tube may be initiated with or without presence of slippage between steel and concrete. Slippage indicates the bulging formation of the specimen without internal work of the concrete infill and in case of proper confinement, failure occurred without slippage by the lateral expansion of the concrete.

iv. The stub column specimens (C7, C8) showed local buckling and concrete crushing at failure. Besides the local buckling in the tube, fracture was observed in column C8. The reasons for the fracture mainly lie in three aspects: (1) large axial deformation; (2) welding quality; and (3) residual stress generated from the welding process. Tensile stresses are induced in the welded region and compression stresses are developed in the region far from the weld. The developed tensile stresses generally provide the driving force to the crack generation.

Table 4.1 Failure modes of test columns

Specimen design	Cross-sectional size	Concrete compressive strength	Yield stress	Cross-sectional slenderness	Overall slenderness	Failure pattern
	B x t x L	$f_c^/$	f_y	B/t	L/B	
	(mm x mm x mm)	(MPa)	(MPa)			
C1	100 x 4 x 1000	27	350	25	10	Global buckling
C2	100 x 4 x 1000	35	350	25	10	Global buckling
C3	100 x 4 x 1000	44	350	25	10	Global buckling
C4	125 x 3 x 1000	35	350	42	8	Outward local buckling
C5	125 x 4 x 1000	35	350	31	8	Outward local buckling
C6	125 x 5 x 1000	35	350	25	8	Outward local buckling
C7	100 x 4 x 500	35	350	25	5	Outward local buckling
C8	100 x 4 x 300	35	350	25	3	Welding failure
C9	150 x 4 x 1000	35	350	37.5	6.6	Outward local buckling
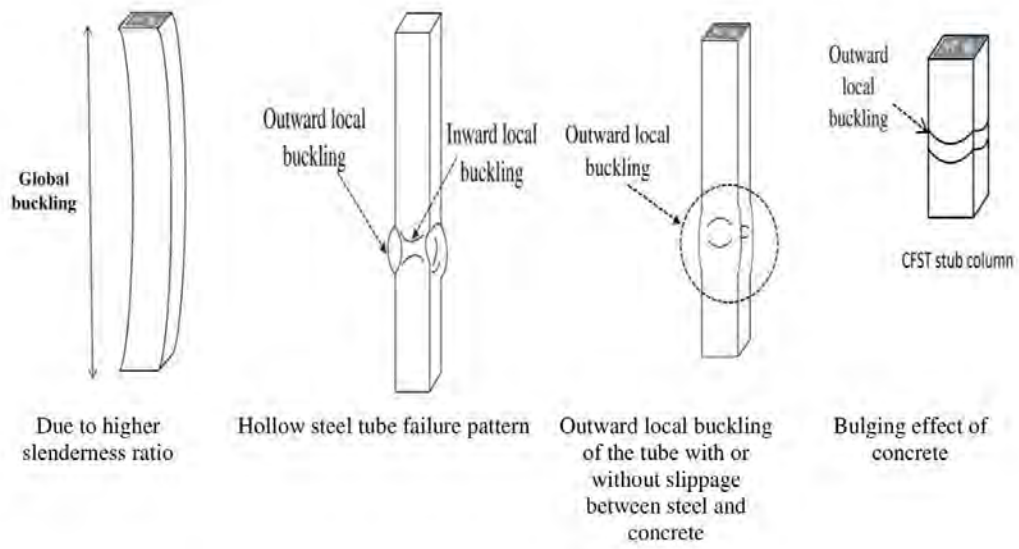
Figure 4.1 Typical failure modes of CFST column.
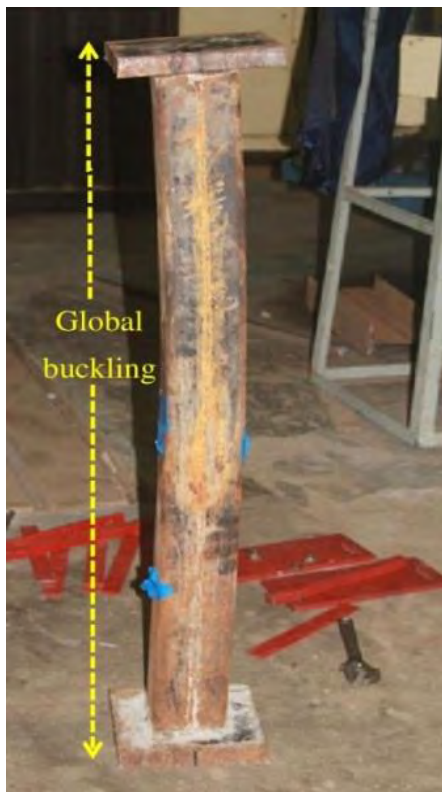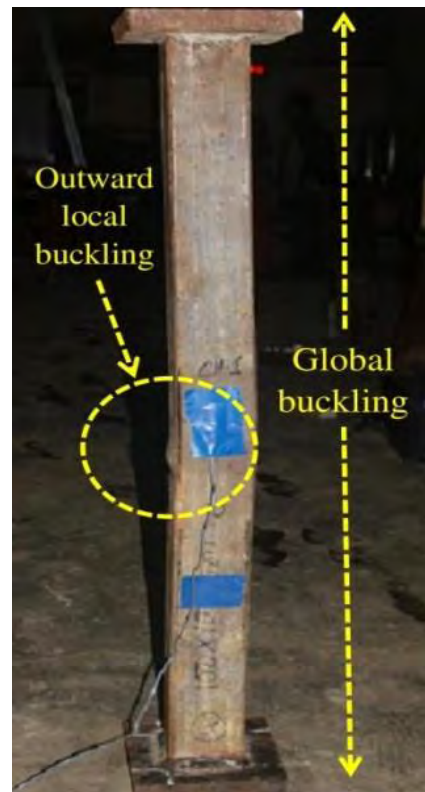
(a) C1 and C2 (L/B = 10) (b) C3 (L/B = 10)

(C) C4, C5 and C6 (B = 125 mm)
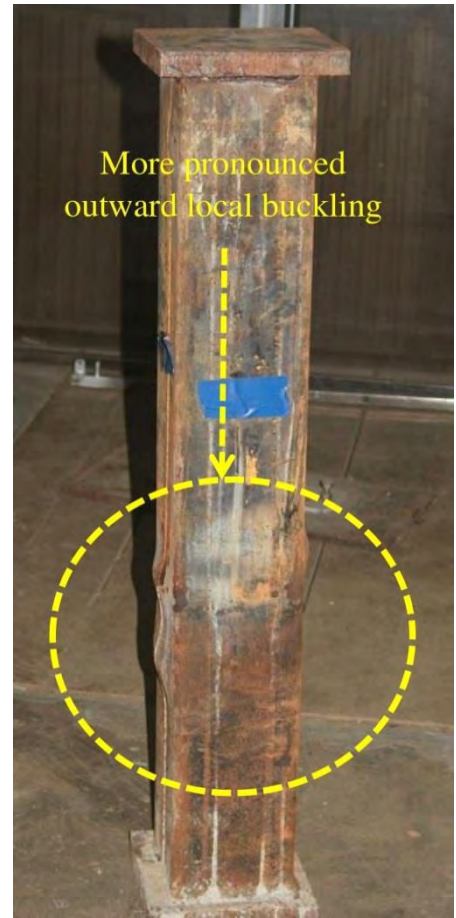
(d) C9 (B = 150 mm)

(e) C7 (L = 500 mm)

(f) C8 (L = 300 mm)

4.3 Axial load versus axial strain relation

The effect of concrete compressive strength ($f_c^/$), plate slenderness ratio (B/t) and global slenderness ratio (L/B) on the measured axial load (*N*) versus axial strain (ε) curves is shown in Figures 4.3, 4.4 and 4.5 respectively. In the figures, the axial loads were calculated from the testing machine and axial strains were calculated from the average value of strain gauges and LVDTs. To measure the strains: strain gauges were used before tube buckling and after that, displacement readings of the LVDTs were divided by the length of the specimens (Yu et al. 2016). The steel yield strains obtained from the steel coupon tests are also indicated in the figures. Additionally, the moment when the initial local buckling was observed is marked by a solid circle on the load-strain curve shown in Figures 4.3, 4.4 and 4.5 for each specimen. Columns developed local buckling at a load level of about 90% of the peak loads. This indicates that the steel tubes buckled after yielding of steel.

4.3.1 Effect of concrete compressive strength ($f_c^/$)

It can be seen from Figure 4.3 that, the ascending curves of the specimens become steeper with the increase of concrete strength. It indicates that as the concrete strength increased, the stiffness of the specimens increased. It can also be seen that the local buckling occurred earlier in the specimens with lower strength concrete. This may be explained by the earlier and quicker volumetric expansion of lower strength concrete. The descending branch represents gradual decrease of the peak load for lower strength concrete and specimens with higher strength concrete showed sudden drop from the peak load.

Figure 4.3 Effect of Concrete compressive strength on axial load versus axial strain.

4.3.2 Effect of cross-sectional slenderness ratio (B/t)

The effect of B/t ratio on the load-strain curves are illustrated in Figure 4.4. The figure shows that increasing the B/t ratio reduced their initial stiffness. This is attributed to the fact that a column with a larger B/t ratio had a lesser steel area. Since, the specimens with higher B/t ratio also experienced earlier local buckling than the specimens having higher B/t ratio. Specimens with lower B/t ratio exhibited better deformation capacity due to its greater lateral support to the concrete core.
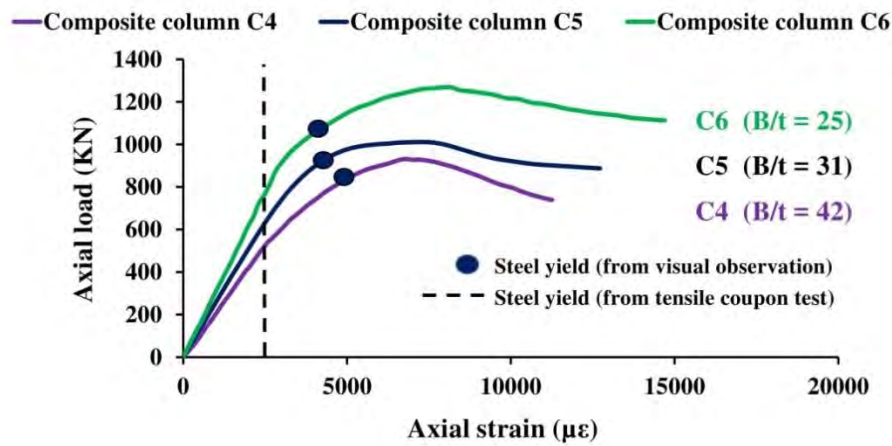
Figure 4.4 Effect of cross-sectional slenderness ratio on axial load versus axial strain

4.3.3 Effect of global slenderness ratio (L/B)

The effect of global slenderness ratio was observed considering different length of the specimens as shown in Figure 4.5. Columns with higher slenderness ratio was shown to have greater flexibility which resulted lower stiffness compared to column with lower slenderness ratio.
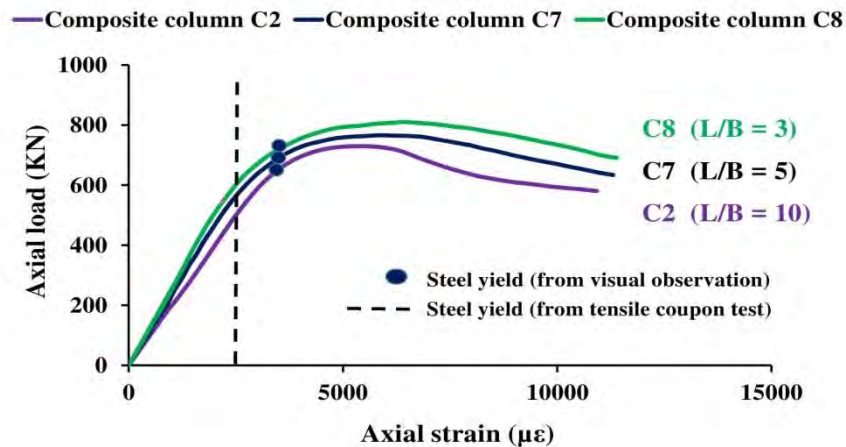
Figure 4.5 Effect of global slenderness ratio on axial load versus axial strain.

4.4 Axial strain at peak load

Axial strain at peak load is a great indicator of confinement and deformability as well as ductility of the specimen which is very interesting parameter in design consideration. The effect of concrete compressive strength (f_c'), plate slenderness ratio (B/t) and global slenderness ratio (L/B) on the peak strain is shown in Table 4.2.

Table 4.2 Axial strain at peak load of test columns

Specimen design	Cross-sectional size	Concrete compressive strength	Yield stress	Cross-sectional slendeness	Overall slenderness	Strain at peak load	% of variation
	B x t x L	f_c'	f_y	B/t	L/B	ε_u	% $\Delta\varepsilon_u$
	(mm x mm x mm)	(MPa)	(MPa)			($\mu\varepsilon$)	
C1	100 x 4 x 1000	27	350	25	10	7098	−
C2	100 x 4 x 1000	35	350	25	10	5619	− 21%
C3	100 x 4 x 1000	44	350	25	10	5571	− 22%
C6	125 x 5 x 1000	35	350	25	8	8143	−
C5	125 x 4 x 1000	35	350	31	8	7204	− 12%
C4	125 x 3 x 1000	35	350	42	8	6706	− 18%
C2	100 x 4 x 1000	35	350	25	10	5619	−
C7	100 x 4 x 500	35	350	25	5	5956	+ 6%
C8	100 x 4 x 300	35	350	25	3	6359	+ 14%

4.4.1 Effect of concrete compressive strength (f_c')

It can be seen from Figure 4.6, that a specimen comprised of high strength concrete generally has a smaller peak strain compared with the corresponding specimen in-filled with lower strength concrete. It is not surprising since high-strength concrete dilates much slower than normal strength concrete.

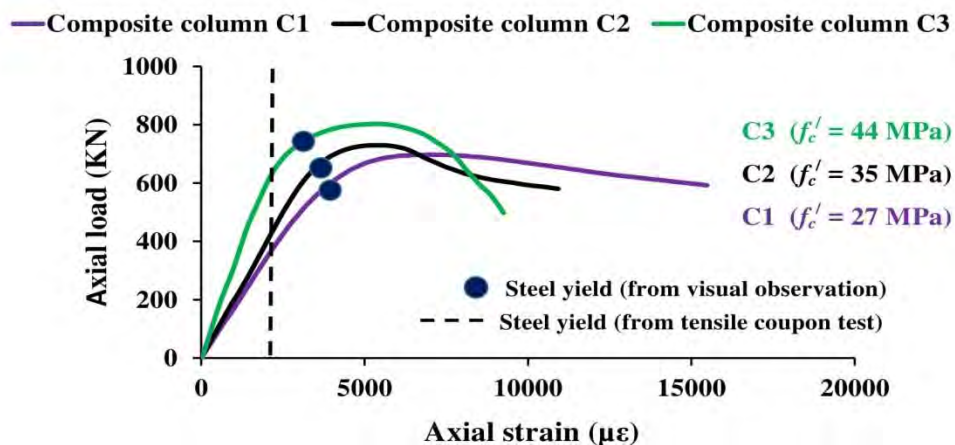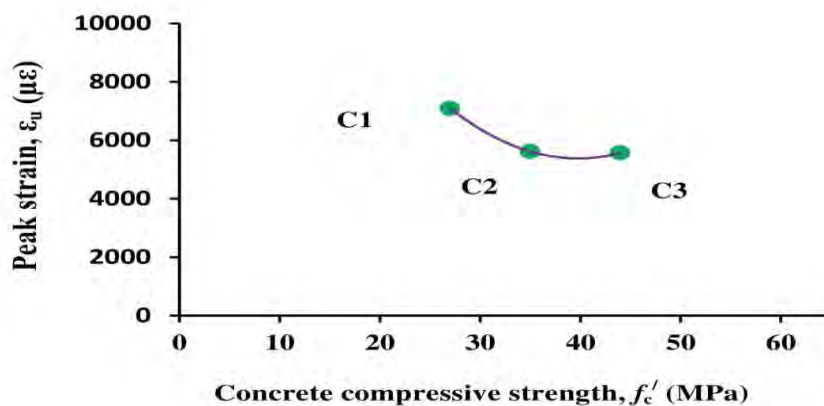**Figure 4.6** Effect of concrete compressive strength on peak strain.

4.4.2 Effect of cross-sectional slenderness ratio (B/t)

Figure 4.7 demonstrates the influence of B/t ratio on the axial strain at load of tested columns. The values of peak strain increased with the decrease of B/t ratio.
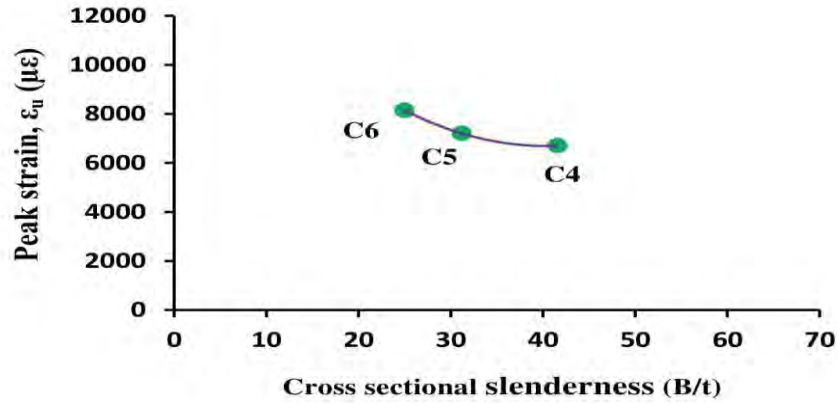
Figure 4.7 Effect of cross-sectional slenderness ratio on peak strain.

This is attributable to the fact that thicker steel tube can delay the local buckling of the tube thus delay the local buckling of the steel tube effectively and thus increase the strain.

4.4.3 Effect of global slenderness ratio (L/B)

The effect of global slenderness ratio on the ultimate axial strain is shown in Figure 4.8. The value of peak strain decreased with increasing slenderness ratio. This is because a column with a larger L/B ratio failed at a smaller load level and the materials had not fully utilized.
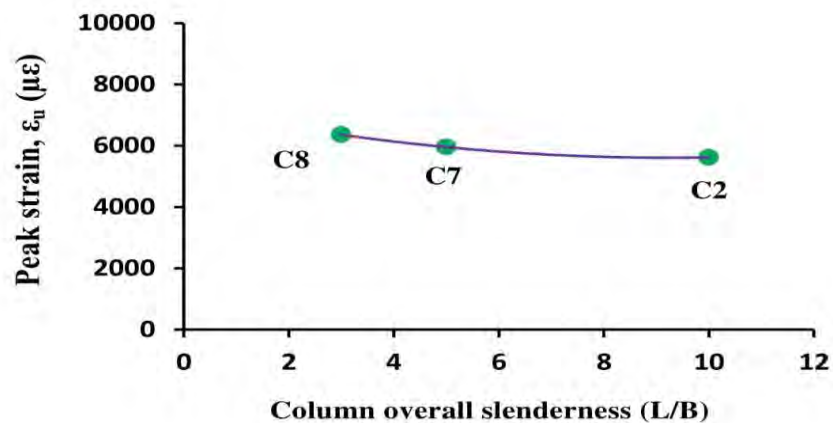
Figure 4.8 Effect of global slenderness ratio on peak strain.

4.5 Ultimate Load

The maximum load during loading is defined as the ultimate load. The ultimate load of the specimens is shown in Table 4.3.

Table 4.3 Ultimate load of test columns

Specimen design	Cross-sectional size	Concrete compressive strength	Yield stress	Cross-sectional slendeness	Overall slenderness	Ultimate load	% of variation
	B x t x L	$f_c^{/}$	f_y	B/t	L/B	P_u	% ΔP_u
	(mm x mm x mm)	(MPa)	(MPa)			(kN)	
C1	100 x 4 x 1000	27	350	25	10	697	–
C2	100 x 4 x 1000	35	350	25	10	729	+ 5%
C3	100 x 4 x 1000	44	350	25	10	804	+ 15%
C6	125 x 5 x 1000	35	350	25	8	1269	–
C5	125 x 4 x 1000	35	350	31	8	1011	– 21%
C4	125 x 3 x 1000	35	350	42	8	930	– 27%
C2	100 x 4 x 1000	35	350	25	10	729	–
C7	100 x 4 x 500	35	350	25	5	770	+ 6%
C8	100 x 4 x 300	35	350	25	3	810	+ 11%

4.5.1 Effect of concrete compressive strength ($f_c^{/}$)

Figure 4.9 shows the effects of concrete compressive strengths ranging from 27 to 44 MPa on the ultimate axial strengths of CFST columns. It can be seen from Figure 4.9 that increasing the concrete compressive strength significantly increases the ultimate axial strengths of the columns. When increasing the concrete compressive strength from 27 MPa to 35 MPa and 44 MPa, the ultimate axial strength is found to increase by 4.9% and 15.35% respectively.
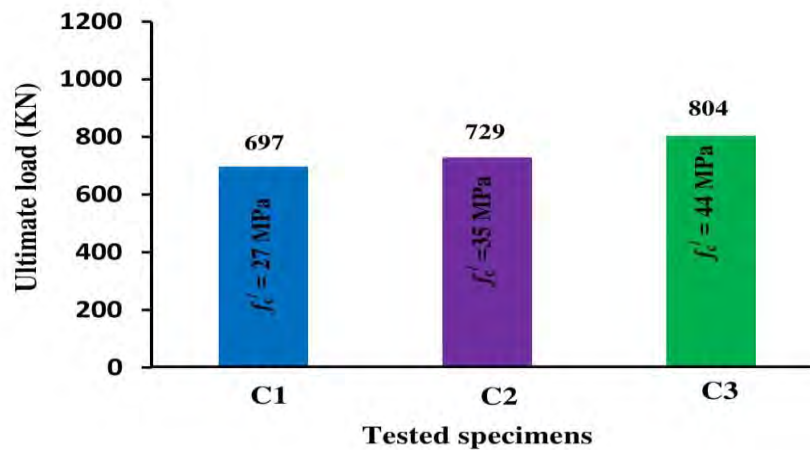
Figure 4.9 Effect on concrete compressive strength on ultimate load.

4.5.2 Effect of cross-sectional slenderness ratio (B/t)

The effects of B/t ratio ranging from 25 to 42 on the ultimate axial loads of CFST columns are demonstrated in Figure 4.10. The figure illustrates that decreasing the B/t ratio remarkably increases the ultimate axial loads of CFST columns. When the B/t ratio decreases from 42 to 31 and 25, the ultimate axial strength of the columns increase by 8.70% and 36.45% respectively.
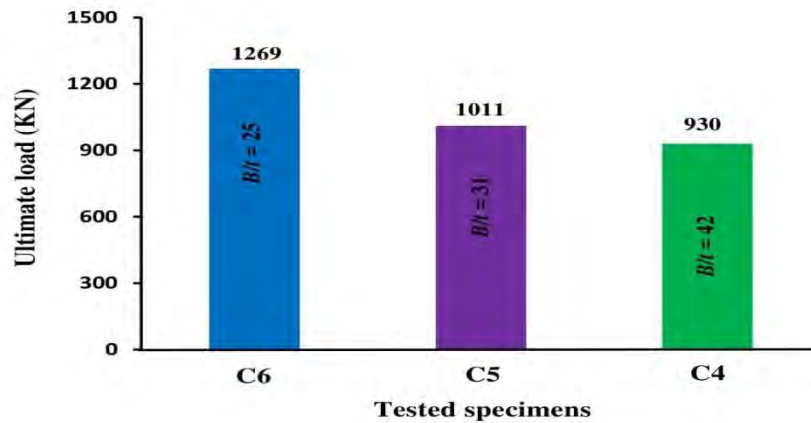
Figure 4.10 Effect of cross-sectional slenderness ratio on ultimate load.

4.5.3 Effect of global slenderness ratio (L/B)

The relationship between the ultimate axial strength and the column slenderness ratio ranging from 3 to 10 is demonstrated in Figure 4.11. It would appear from Figure 4.11 that increasing the column slenderness ratio causes a significant reduction in the ultimate axial load. When the L/B ratio decreases from 10 to 5 and 3, the ultimate axial strength of the columns increase by 5.62% and 11.12% respectively.
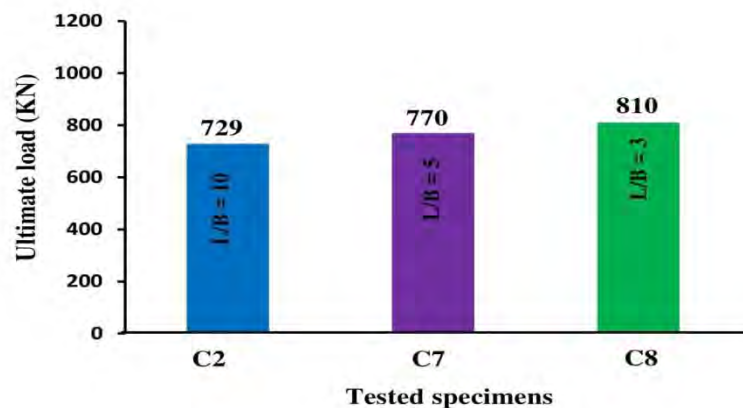
Figure 4.11 Effect of global slenderness ratio on ultimate load

4.6 PERFORMANCE INDICIES

Performance indices are used to evaluate the contributions of the concrete and steel components to the ultimate strengths of CFST columns and to quantify the strength reduction caused by the section, column slenderness and initial geometric imperfections. These performance indices can be used to investigate the cost effective designs of CFST under biaxial loads. The performance indexes such as ductility index, concrete contribution ratio and strength index were determined to observe the performance and cost effective design of CFST column.

4.6.1 Ductility index

"Ductility" often refers to the ability of a structure to sustain deformation beyond the elastic limit while maintaining a reasonable load carrying capacity until total failure. In modern seismic codes of practice, like EC8 (Eurocode 8, 2005), it is very common to design ductile structures to drastically reduce the design seismic force, leading to a more economical design. The influence of other extreme events, like blast, impact, cyclone and fire, on structures can also be mitigated if the structures are ductile. Currently, the design of ductile structures is to a large extent based on prescriptive detailing provisions.

According to Ren et al. 2018, Ductility indexing is defined as the ratio of axial shortening at ultimate strength and post peak shortening corresponding to 85% of the ultimate strength as shown in Figure 4.12. The ductility index of the test specimens is shown in Table 4.4.
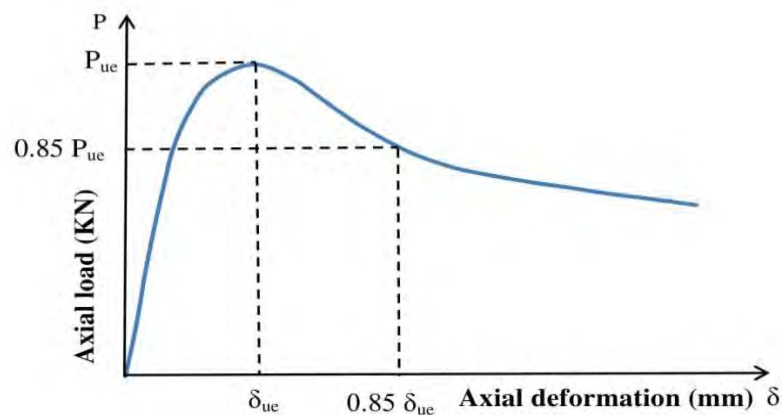
Figure 4.12 Definition of ductility index (DI).

Table 4.4 Ductility index of test columns

Specimen design	Cross-sectional size	Concrete compressive strength	Yield stress	Cross-sectional slendeness	Overall slenderness	Ductility index	% of variation
	B x t x L	$f_c^{/}$	f_y	B/t	L/B	D.I.	% ΔD.I.
	(mm x mm x mm)	(MPa)	(MPa)				
C1	100 x 4 x 1000	27	350	25	10	2.18	—
C2	100 x 4 x 1000	35	350	25	10	1.51	− 31%
C3	100 x 4 x 1000	44	350	25	10	1.31	− 40%
C6	125 x 5 x 1000	35	350	25	8	2.00	—
C5	125 x 4 x 1000	35	350	31	8	1.80	− 10%
C4	125 x 3 x 1000	35	350	42	8	1.55	− 22%
C2	100 x 4 x 1000	35	350	25	10	1.51	—
C7	100 x 4 x 500	35	350	25	5	1.69	+ 12%
C8	100 x 4 x 300	35	350	25	3	1.81	+ 20%

4.6.1.1   Effect of concrete compressive strength ($f_c^{/}$)

It can be observed from Figure 4.13 that the columns filled with lower strength concrete exhibited higher DI than that of lower strength concrete. As discussed earlier, high strength infill concrete specimen drops the peak load rapidly, resulting less deformation capacity as well as ductility.
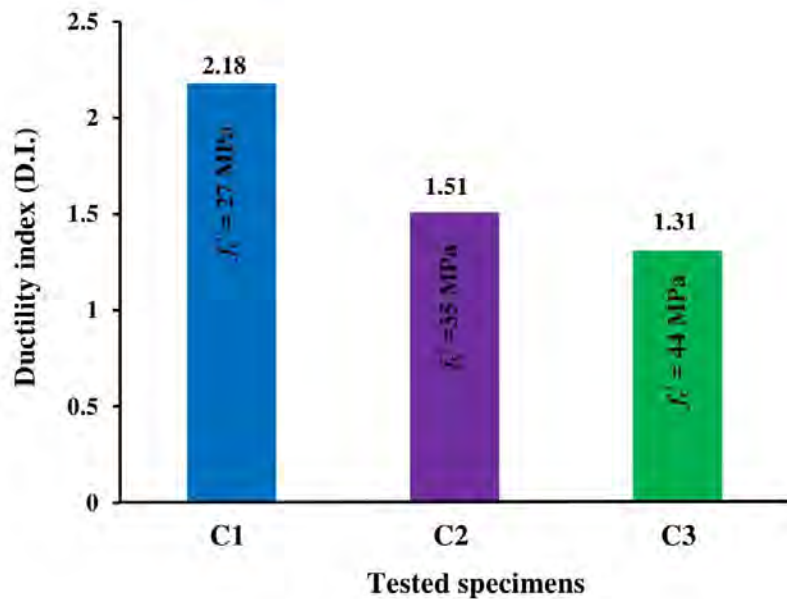
Figure 4.13 Effect of concrete compressive strength on ductility index.

4.6.1.2 Effect of cross-sectional slenderness ratio (B/t)

Most influential parameter of changing DI is steel contribution of the tested specimen. It can be seen from Figure 4.14 that DI of a specimen increased with the decrease of the cross sectional width to thickness ratio of the specimen. This may be attributed due to the gradual decrease of peak load of high steel contributed specimen.
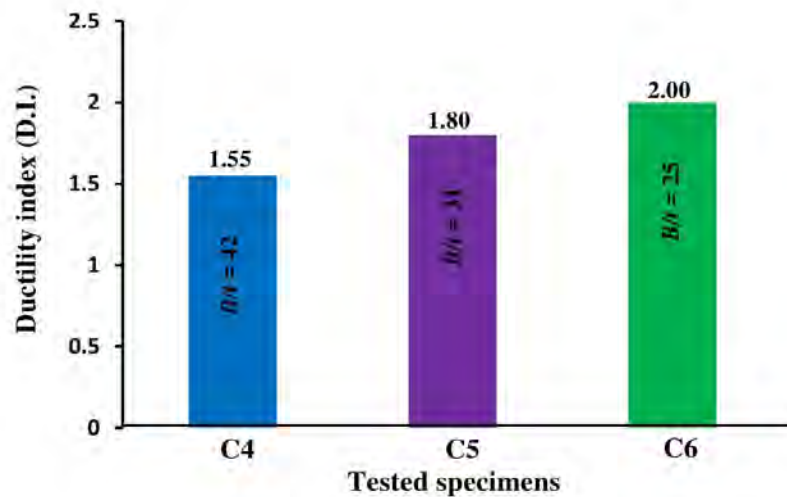
Figure 4.14 Effect of cross-sectional slenderness ratio on ductility index.

4.6.1.3 Effect of global slenderness ratio (L/B)

In Figure 4.15, specimens of higher L/B ratio showed lower DI, since plasticity and confinement of a specimen decrease with the increase of the length of a specimen.
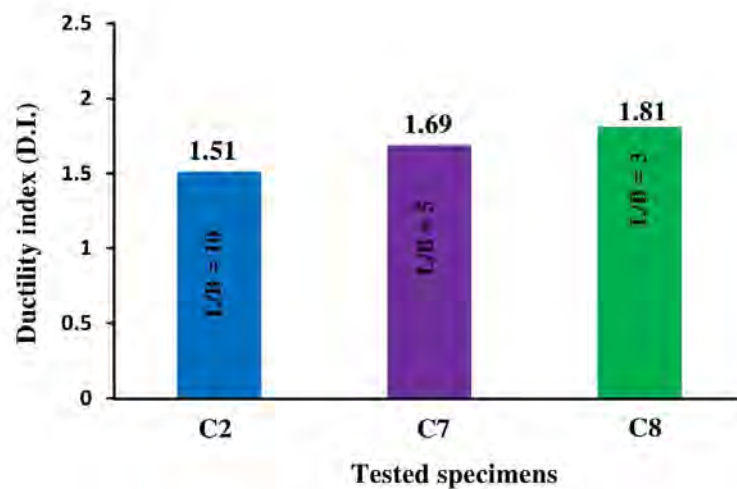
Figure 4.15 Effect of global slenderness ratio on ductility index.

4.6.2 Concrete contribution ratio

The concrete contribution ratio quantifies the contribution of the concrete component to the ultimate axial strength of a CFST column. The concrete core column without reinforcement carries very low loading and does not represents the concrete core in a CFST column. (Portolés et al. 2011) used the capacity of the hollow steel tubular column to define the concrete contribution concrete contribution ratio (CCR), which is given by, Concrete contribution ratio (ξ_c) = P_u / $A_s f_y$

Where,

$A_s f_y$ = load of corresponding hollow steel

P_u = Ultimate load of the tested column

Table 4.5 presents concrete contribution ratio of test columns. This table also shows the effects of concrete compressive strength ($f_c^/$), cross-sectional slenderness ratio (B/t) and global slenderness ratio (L/B) on the concrete contribution of the CFST columns.

Table 4.5 Concrete contribution ratio of test columns

Specimen design	Cross-sectional size	Concrete compressive strength	Yield stress	Cross-sectional slendeness	Overall slenderness	Concrete contribution ratio	% of variation
	B x t x L	$f_c^/$	f_y	B/t	L/B	ξ_C	% $\Delta \xi_c$
	(mm x mm x mm)	(MPa)	(MPa)				
C1	100 x 4 x 1000	27	350	25	10	1.31	–
C2	100 x 4 x 1000	35	350	25	10	1.37	+ 5%
C3	100 x 4 x 1000	44	350	25	10	1.51	+ 15%
C6	125 x 5 x 1000	35	350	25	8	1.46	–
C5	125 x 4 x 1000	35	350	31	8	1.51	+ 3%
C4	125 x 3 x 1000	35	350	42	8	1.83	+ 25%
C2	100 x 4 x 1000	35	350	25	10	1.37	–
C7	100 x 4 x 500	35	350	25	5	1.33	– 3%
C8	100 x 4 x 300	35	350	25	3	1.29	– 6%

4.6.2.1 Effect of concrete compressive strength ($f_c^/$)

The concrete contribution ratios of CFST columns with concrete compressive strengths ranging from 27 to 44 MPa are given in Figure 4.16. The Figure demonstrates that increasing the concrete compressive strength significantly increases the concrete contribution ratio. This implies that the axial strength performance of a CFST column can be improved significantly by using high strength

concrete as infill. The calculated concrete contribution ratio for the concrete compressive strength of 27 MPa, 35 MPa and 44 MPa is 1.31, 1.37 and 1.51 respectively.
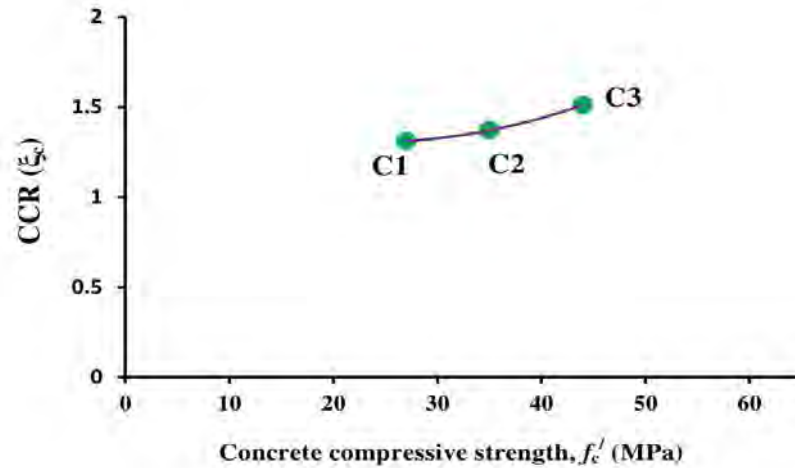
Figure 4.16 Effect of concrete compressive strength on concrete contribution ratio.

4.6.2.2 Effect of cross-sectional slenderness ratio (B/t)

The effects of the B/t ratio ranging from 25 to 42 on the concrete contribution ratio of concentrically loaded CFST columns are shown in Figure 4.17. The concrete contribution ratio is found to increase significantly with an increase in the B/t ratio. This may be explained by the fact that increasing the B/t ratio reduces the axial load capacity of the steel tube and increases the cross-sectional area of the concrete core, thereby increasing the contribution of the concrete component.
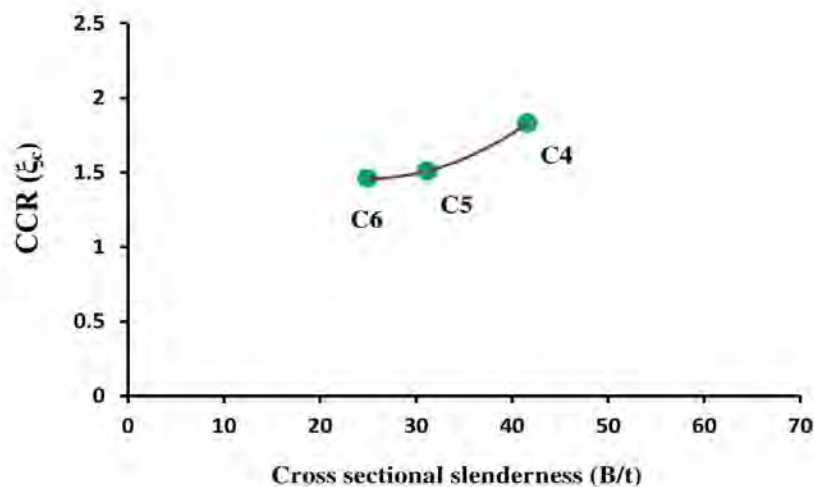
Figure 4.17 Effect of cross-sectional slenderness ratio on concrete contribution ratio.

4.6.2.3 Effect of global slenderness ratio (L/B)

Figure 4.18 presents the results of the concrete contribution ratios calculated by varying the column slenderness ratios ranging from 3 to 10.
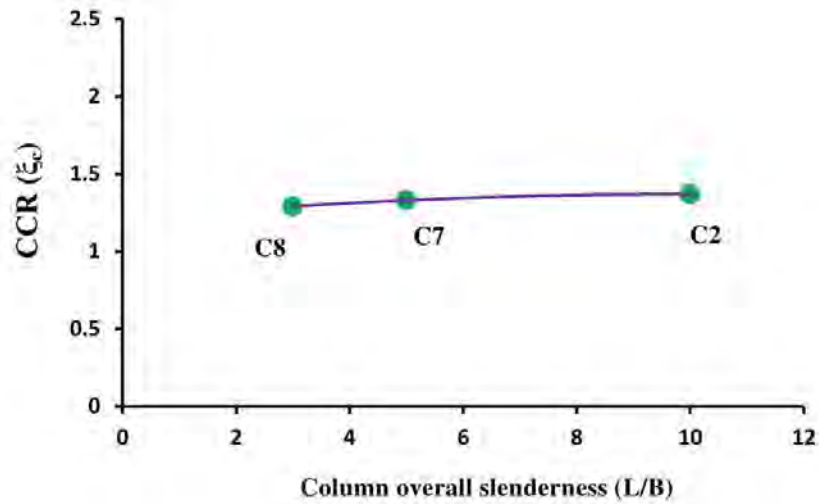
Figure 4.18 Effect of global slenderness ratio on concrete contribution ratio.

It appears that the concrete contribution of CFST decreases when increasing the column slenderness ratio.

4.6.3 Strength index (SI)

For convenience of analysis, a strength index (SI) defined by Han et al. 2017 is used herein to quantify the ultimate strength as:

Strength index (SI) = P_u / P_0

Where,

P_u = Ultimate load of the tested column

$P_0 = A_s f_y + A_c f_c'$

Table 4.6 presents Strength index (SI) of test columns. This table also shows the effects of concrete compressive strength (f_c'), cross-sectional slenderness ratio (B/t) and global slenderness ratio (L/B) on the strength index (SI) of the CFST columns.

Table 4.6 Strength index (SI) of test columns

Specimen design	Cross-sectional size	Concrete compressive strength	Yield stress	Cross-sectional slendeness	Overall slenderness	Strength index (SI)	% of variation
	B x t x L	$f_c^/$	f_y	B/t	L/B	P_{exp}/P_{th}	% $\Delta P_{exp}/P_{th}$
	(mm x mm x mm)	(MPa)	(MPa)				
C1	100 x 4 x 1000	27	350	25	10	0.92	–
C2	100 x 4 x 1000	35	350	25	10	0.89	– 3%
C3	100 x 4 x 1000	44	350	25	10	0.88	– 4%
C6	125 x 5 x 1000	35	350	25	8	1.00	–
C5	125 x 4 x 1000	35	350	31	8	0.96	– 4%
C4	125 x 3 x 1000	35	350	42	8	0.93	– 7%
C2	100 x 4 x 1000	35	350	25	10	0.89	–
C7	100 x 4 x 500	35	350	25	5	0.93	+ 4%
C8	100 x 4 x 300	35	350	25	3	0.98	+ 10%

4.6.3.1   Effect of concrete compressive strength ($f_c^/$)

As shown in Figure 4.19, SI decreases by 3% and 4% when concrete compressive strength increases from 27 MPa to 35 MPa and 44 MPa. This may be attributed to the fact that the confining effect by the steel tube for higher strength concrete filled tube columns is much less than the medium or low strength concrete ones. When the concrete compressive strength is increased from 27 MPa to 35 MPa and 44 MPa, the strength index (SI) is found to be reduced from 0.92 to 0.89 and 0.88 respectively.
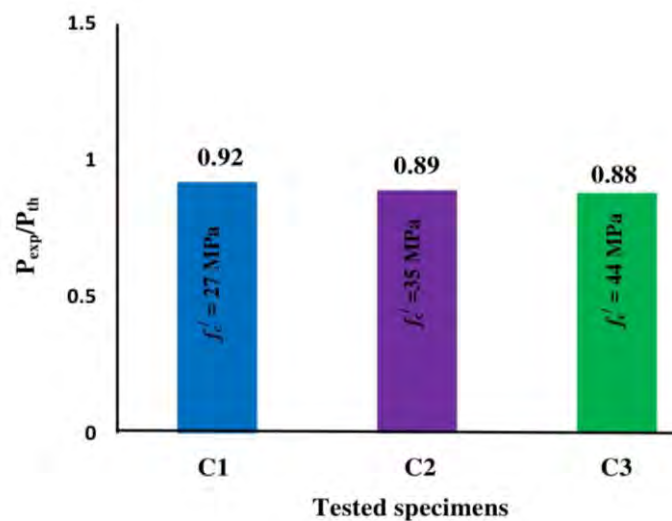
Figure 4.19 Effect of concrete compressive strength on strength index (SI).

4.6.3.2 Effect of cross-sectional slenderness ratio (B/t)

Figure 4.20 demonstrates the effects of the B/t ratio ranging from 25 to 42 on the strength index (SI) of test columns. It can be observed from the figure 4.20 and table 4.6 that the strength index (SI) decreases by 4% and 7% with an increase in the B/t ratio from 25 to 31 and 42 of the same size cross-section. It is known that increasing the B/t ratio causes a greater difference between the experimental and theoretical strengths of the CFST columns because of the lesser support of the thinner steel tube to the concrete core.
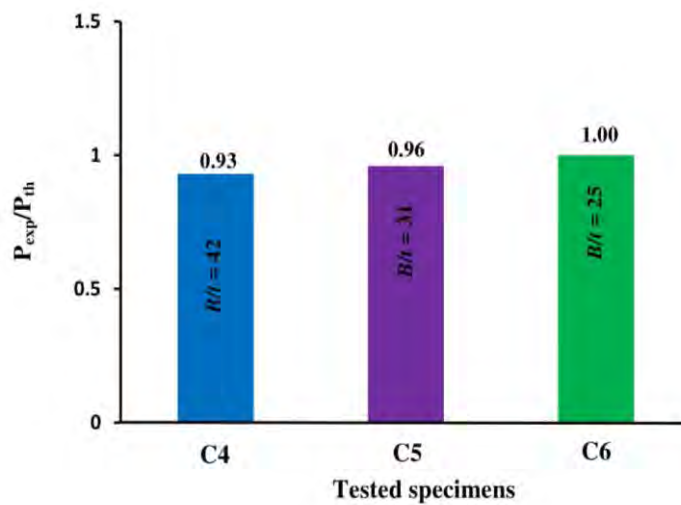
Figure 4.20 Effect of cross-sectional slenderness ratio on strength index (SI)..

4.6.3.3 Effect of global slenderness ratio (L/B)

The strength index (SI) of the columns were determined by varying the column slenderness ratio ranging from 3 to 10 and the results are presented in figure 4.21.
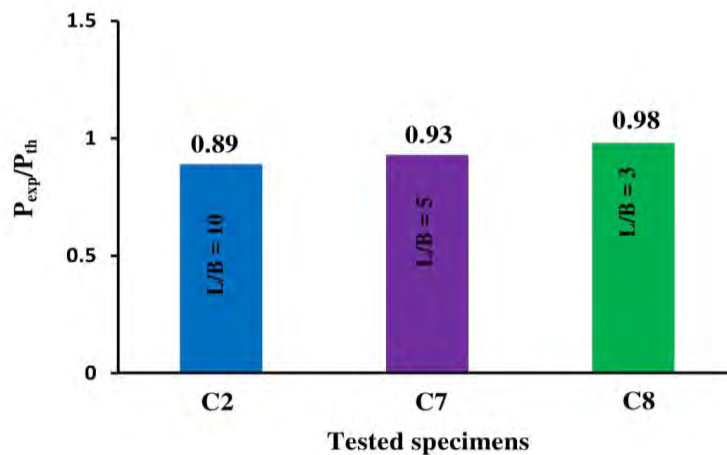
Figure 4.21 Effect of global slenderness ratio on strength index (SI).

The figure indicates that the column slenderness has a pronounced effect on the ultimate axial strengths of CFST columns. The strength index (SI) is significantly reduced by increasing the column slenderness ratio. This is because of the fact that the columns having higher overall slenderness ratio, buckle much earlier before gaining its full capacity.

It can be seen from table 4.6, that most of test column presents the value of strength index (SI) is below 1. According to the definition of strength index (SI) it indicates that the experimental capacity of test columns is lower than theoretical capacity. This is because of the less confinement effect in the square CFST columns. To overcome this problem a strength reduction factor may be included in the design codes of square CFST column.

4.7   Summary

A detailed experimental investigation was performed to study the behavior of CFST columns under concentric loading. The geometric and material properties were varied and their influence was observed with respect to failure modes, ultimate load, load strain responses and performance indexes. Based on the results, it was determined that concrete compressive strength, cross sectional slenderness ratio and global slenderness ratio have significant effect on the fundamental behavior of CFST column. Increasing the concrete compressive strength improved the ultimate capacity of the column but decreased the overall column performance because of its less ductile behavior. On the other hand, columns with higher global slenderness ratio showed lower ultimate capacity and less ductile behavior with global buckling failure. Column with lower cross sectional slenderness ratio exhibited better column performance for its higher steel contribution of the specimens but columns with higher cross sectional slenderness ratio showed outward local buckling failure mode. The positive effect of the confinement is not observed for the tested columns and the theoretical sectional capacity overestimated the real capacity.

CHAPTER 5
DESIGN CODES AND COMPARISIONS

5.1 General

Different formulae were proposed over the years to calculate the axial capacity of the CFST columns. For instance, some of them accounted for the increase in the in filled concrete strength while other just ignored it. Conceptually, the American Concrete Institute ACI-318 (2014) uses the concept of reinforced concrete design in their formulation without any consideration to the concrete confinement effects. The American Institute of Steel Construction AISC (2010) formula is based on the structural steel. While the exclusively used for composite elements design, Eurocode-4 (2005) combine both these approaches. In this chapter, the design approaches adopted in (Eurocode 4, AISC-LRFD 2010, ACI 2014 and Wang et al. 2016) are reviewed and applied to calculate the ultimate strength of the tests columns. Subsequently, the predicted values are compared with the experimental results obtained from the experiments.

5.2 AISC-LRFD (2010) Formulae

The AISC-LRFD (2010) defines a composite column as a steel column fabricated from rolled or built-up steel shapes and encased in structural concrete or fabricated from steel pipe or tubing and filled with structural concrete. In this specification, the design method for composite columns is based on the ultimate strength of the materials part of the cross-section and takes into account the inelastic material properties with the required design loads as factored service loads. It contains the latest design approach of structural steel based on the ultimate strength concept. The nominal strength of a composite cross section is calculated from the ultimate resistance to load and reduction capacity factors related to material properties and characteristics of member failure are applied to the nominal strength of the cross-section.

For the plastic stress distribution method, the nominal strength shall be computed assuming steel components have reached a stress of f_y in either tension or compression and concrete components in compression due to axial force and/or flexure have reached a stress of $0.85f_c'$. For round HSS filled with concrete, a stress of $0.95f_c'$ is permitted to be used for concrete components in compression due to axial force and/or flexure to account for the effects of concrete confinement.

Local buckling of the CFST should be accounted for through classification of these composite members into compact, non-compact or slender. The element is considered to be compact if its b/t ratio is less than λ_p and to be non-compact if its b/t ratio is more than λ_p but less than λ_r. Moreover, if the section's ⁄ratio exceeds, then it is classified as slender. The maximum allowed ⁄ratio specified in the Table 5.1 should not be exceeded in order for the AISC's formulae to be applicable. Table 5.2 shows the limits of b/t ratios for CFST members subject to axial compression and their calculation for local buckling classification. Based on these limits, all the tested sections in this study are compact.

Table 5.1 The condition for compact, noncompact and slender composite member subjected to axial compression (AISC-2010)

Description of Element	Width to thickness Ratio	λ_p Compact/Noncompact	λ_r Noncompact/Slender	Maximum Permitted
Walls of Rectangular HSS and Boxes of uniform Thickness	b/t	$2.26\sqrt{\dfrac{E}{F_y}}$	$3.00\sqrt{\dfrac{E}{F_y}}$	$5.00\sqrt{\dfrac{E}{F_y}}$
Round HSS	D/t	$\dfrac{0.15\,E}{F_y}$	$\dfrac{0.19\,E}{F_y}$	$\dfrac{0.31\,E}{F_y}$

The compressive capacity of axially loaded circular concrete filled steel tubes can be determined for the limit state of flexural buckling with the following equations for compact sections: $P_u = f_y A_s + C_2 f_c' A_c$ (5.1)

Where,

$C_2 = 0.85$ for rectangular section and 0.95 for circular section.

The effective stiffness of the composite section, EI_{eff}, for all section shall be:

$$EI_{eff} = E_sI_s + E_sI_{sr} + C_3E_cI_c \tag{5.2}$$

Where, C_3 = coefficient for calculation of effective rigidity of filled composite compression member.

$$C_3 = 0.6 + 2\left[\frac{A_s}{A_s+A_c}\right] \le 0.9 \tag{5.3}$$

Table 5.2 Compactness check of test columns

Specimen design.	Cross-sectional size	Width to thickness Ratio	λ_p	λ_r	Maximum Permitted	Type of cross-sectional slenderness
	B x t x L	b/t				
	(mm x mm x mm)					
C1	100 x 4 x 1000	23	54	72	119	Compact
C2	100 x 4 x 1000	23	54	72	119	Compact
C3	100 x 4 x 1000	23	54	72	119	Compact
C4	125 x 3 x 1000	39.7	54	72	119	Compact
C5	125 x 4 x 1000	29.2	54	72	119	Compact
C6	125 x 5 x 1000	23	54	72	119	Compact
C7	100 x 4 x 500	23	54	72	119	Compact
C8	100 x 4 x 300	23	54	72	119	Compact
C9	150 x 4 x 1000	35.5	54	72	119	Compact

The available compressive strength need not be less than specified for the bare steel member

$$P_e = \frac{\pi^2 EI_{eff}}{(KL)^2} \tag{5.4}$$

A_c = Area of concrete, in^2 (mm^2)

A_s = Area of the steel section, in^2 (mm^2)

E_c = Elasticity modulus of concrete = $W_c^{1.5}\sqrt{f'c}$, Ksi / $\left(0.043W_c^{1.5}\sqrt{f'c}\right)$, Mpa

EI_{eff} = Effective stiffness of composite section, kip-in^2 (N-mm^2)

E_s = Modulus of elasticity of steel = 29,000 ksi (200,000 MPa)

f_y = Specified minimum yield stress of steel section, ksi (MPa)

f_{ysr} = Specified minimum yield stress of reinforcing bars, ksi (MPa)

I_c = Moment of inertia of the concrete section about the elastic neutral axis of the composite section, in^4 (mm^4).

I_s = Moment of inertia of steel shape about the elastic neutral axis of the composite section, in^4 (mm^4)

I_{sr} = Moment of inertia of reinforcing bars about the elastic neutral axis of the composite section, in^4 (mm^4)

K = effective length factor

L = laterally unbraced length of the member, in (mm)

$f_c^/$ = specified compressive strength of concrete, ksi (MPa)

W_c = weight of concrete per unit volume ($90 \leq W_c \leq 155$ lbs/ft3 or $1500 \leq W_c \leq 2500$ kg/m³)

The design compressive strength, ϕcPn of doubly symmetric axially loaded concrete filled composite members shall be determined for the limit state of flexural buckling based on member slenderness as follows:

When $\quad p_{no}/p_e \leq 2.25$

$$p_n = p_{no} [0.658^{p_{no}/p_e}]$$ (5.5)

When $\quad p_{no}/p_e > 2.2$

$$p_n = 0.877[p_e]$$ (5.6)

p_{no} = Nominal compressive strength of axially loaded composite member (kN)

p_e = Elastic critical buckling load (kN)

5.3   ACI-318 (2014) Code Formulae

ACI-318 uses the limit state design format with load factors and capacity reduction factors. The strength of a composite column is computed as for reinforced concrete members. The expression for equivalent stiffness includes a creep factor, and cracked concrete stiffness is considered. Minimum eccentricities are specified to cover construction tolerances. The following sections briefly introduce the concerned strength provisions for the concrete filled steel tubular columns as recommended in the ACI-318 building code (2014). ACI code does not consider the increase in confined concrete's axial capacity as shown:

$$N_u = F_y A_s + 0.85 f_c' A_c \tag{5.7}$$

However, 15% of the concrete segment is reduced to account for its uncertainties. In other words, the compression composite members are considered as regular reinforced concrete in these two codes. To account for local buckling of the structural steel tube, a limiting thickness is specified and, not to be exceeded. The magnitude of this thickness is based on the achievement of yield stress in the empty steel tube when subjected to axial monotonic loading. Moreover, this formula does not differentiate between different cross-sectional shapes.

5.4 Eurocode 4 (2005) Formulae

There are two approaches adopted by the Eurocode 4 (2005) for calculating the axial capacity of concrete filled steel tube columns, the general method and the simplified method. In the general method, the second order effects and imperfections of the compression members are taken into consideration explicitly. This method may be used for members with symmetrical sections, but they are also applicable to non-prismatic axial members. Consequently, appropriate software for numerical computation is essential for the application of the general method. In the simplified method, the European buckling curves for steel columns are utilized. The element's imperfections are implicitly taken into account. Unlike the general method, the simplified one is limited to prismatic composite axial members with symmetrical sections. Both methods are based on the following assumptions:

a) Flat sections stay flat while the column is deforming due to loading,

b) Till failure, the existence of full interaction between the concrete and steel surfaces is maintained.

In this research, only the simplified method is applied due to its applicability to the tested specimens and the calculation simplicity.

The plastic resistance to compression $N_{pl,Rd}$ of a composite cross-section should be calculated by adding the plastic resistance of its components:

$$N_{pl,Rd} = A_a f_{yd} + A_c f_{cd} \tag{5.8}$$

For members in axial compression, the design value of the normal force N_{Ed} should

satisfy: $\dfrac{N_{Ed}}{\chi N_{pl,Rd}} \leq 1.0$ (5.9)

Where: $N_{pl,Rd}$ is the plastic resistance of the composite section.

χ is the reduction factor for the relevant buckling mode.

$$\chi = \frac{1}{\Phi \sqrt{\Phi^2 - \lambda^{-2}}}$$

$\Phi = 0.5(1 + \alpha\,(\lambda - 0.2) + \lambda_2)$ (5.10)

For concrete filled tubes of circular cross-section, account is taken of increase in strength of concrete caused by confinement provided that the relative slenderness λ does not exceed 0.5 and e/d < 0.1, where e is the eccentricity of loading given by M_{Ed}/N_{Ed} and d is the external diameter of the column.

The plastic resistance to compression is calculated from the following expression:

$$N_{pl,Rd} = \eta_a A_a f_{yd} + A_c f_c d \left(1 + \eta_c \frac{t}{d}\frac{f_y}{f_{ck}}\right)$$ (5.11)

Where: t is the wall thickness of the steel tube, for members with e = 0 the values ηa = η_{ao} and ηc= η_{co} are given by the following expressions:

$\eta_{ao} = 0.25\,(3 + 2\lambda)$ (but 1.0) (5.12)

$\eta_{co} = 4.9 - 18.5\lambda_2 + 17\lambda_2$ (but 0) (5.13)

For high strength concrete with f_{ck} > 50 MPa, the effective compressive strength of concrete accordance with EC2 (EN 1992-1-1, 2004) is determined by multiplying the characteristic strength by a reduction factor η as given below.

η = 1.0 - (f_{ck} - 50)/200 (5.14)

The relative slenderness λ for the plane of bending being considered is given by:

$$\lambda = \sqrt{\frac{N_{p1,RK}}{N_{cr}}}$$ (5.15)

N_{cr} is the elastic critical normal force for the relevant buckling mode, calculated with the effective flexural stiffness $(EI)_{eff}$

Where, K_e is a correction factor that should be taken as 0.6.

I_a, and I_c are the second moments of area of the structural steel section, the un-cracked concrete section for the bending plane being considered.

5.5 Wang et al. (2016) Formulae

Recent research indicates that the concrete confinement effect has not been adequately considered by EC4, thus giving unsafe or conservative predictions for the compressive strength of CFST columns. For this reason, a wide range of simulation data was generated by adopting the finite element model proposed by Tao et al. (2013). Based on regression analysis of the simulated data, new simplified models were proposed by Wang et al. (2016) recently to predict the compressive strength, as well as compressive stiffness and ultimate strain (ductility) for CFST columns.

By considering the confinement effect and contributions from the steel tube and concrete, a simple superposition model is proposed by Wang et al. (2016), as shown in Eq. (5.16) to predict the ultimate strength (Nu) for both circular and rectangular CFST columns:

$$N_u = N_a + N_c = \eta_a A_s f_y + \eta_c A_c f_c^{/} \tag{5.16}$$

Where N_a and N_c are the strength contributions from the steel tube and concrete, respectively; A_s and A_c are the cross-sectional areas of the steel tube and core concrete, respectively; η_a and η_c are new proposed factors to consider the effect of concrete confinement.

For rectangular CFST columns, the new factors of η_a and η_c are given by the following expressions by Eq. (3.17 and 3.18):

$$\eta_a = 0.91 + 7.31 \times 10^{-5} - (1.28 \times 10^{-6} + 2.26 \times 10^{-8} f_y) (D^{/}/t)^2 \tag{5.17}$$

$$\eta_c = 0.98 + 29.5 (f_y)^{-0.48} K_s (t f_y / D^{/} f_c^{/})^{1.3} \tag{5.18}$$

Where $D^{\prime}$ is the equivalent diameter of a rectangular column defined in Eq. (3.19):

$$D^{/} = \sqrt{B^2 + H^2} \tag{5.19}$$

Where B and D are the width and height of a rectangular CFST column.

The equivalent confining coefficient k_s in Eq. (3.18) is used to account for the effective confining area in a rectangular CFST column, which is defined in Eq. (3.20):

$$K_s = (1/3) ((B - 2t)/(D - 2t))^2 \tag{5.20}$$

5.6 Limitations of design standards

For design purposes, all these codes have provided some limitations on material strengths and section slenderness, as summarized in Table 5.3. Beyond those

limitations, the existing codes might give less accurate strength predictions. Even within the limitations, the strength predictions from the existing codes show considerable deviation from the experimental results and the predication accuracy could be further improved.

Table 5.3 Predicted guidelines and limitations

Corresponding guidelines	Cross sectional shape	Prediction of ultimate strength	$f_c^{/}$ (MPa)	f_y (MPa)	H/t (H = Cross-sectional height)
AISC	Rectangular	$P_{AISC} = A_s f_y + 0.85 A_c f_c^{/}$ $P_n = P_{no} [\, 0.659^{\frac{P_{no}}{P_e}} \,]$ $P_e = \pi^2 \, (EI_{eff}) \, / \, (KL)^2$ $EI_{eff} = E_s I_{sy} + E_s I_{sr} + C_3 E_c I_{cy}$ $K = 1.00$	$21 \leq f_c^{/} \leq 70$ Mpa	$f_y \leq 525$ Mpa	$\dfrac{\text{H/t} \leq 2.26}{\sqrt{E_s/f_y}}$
EC4	Rectangular	$P_{EC} = A_s f_y + A_c f_c^{/}$	$20 \leq f_c^{/} \leq 60$ Mpa	$235 \leq f_y \leq 460$ Mpa	$\dfrac{\text{H/t} \leq 52}{\sqrt{235/f_y}}$
ACI	Rectangular	$P_{ACI} = A_s f_y + 0.85 A_c f_c^{/}$	$f_c^{/} \geq 17.2$ Mpa	–	$\text{H/t} \leq \sqrt{3E_s/f_y}$
Wang et al. (2016)	Rectangular	$N_u = \eta_a A_s f_y + \eta_c A_c f_c^{/}$ $\eta_a = 0.91 + 7.31 \times 10^{-5} - (1.28 \times 10^{-6} + 2.26 \times 10^{-8} f_y) (D^{/}/t)^2$ $\eta_c = 0.98 + 29.5 (f_y)^{-0.48} K_s (t f_y / D^{/} f_c^{/})^{1.3}$ $D^{/} = \sqrt{B^2 + H^2}$ $K_s = (1/3) \, ((B - 2t)/(D - 2t))^2$	$13 \leq f_c^{/} \leq 164$ Mpa	$194 \leq f_y \leq 835$ Mpa	$11 \leq \text{H/t} \leq 150$

5.7   Comparison of results with code predictions

In this study, the design approaches adopted in (Eurocode 4, AISC-LRFD 2010, ACI 2014 and Wang et al. 2016) were applied to predict the ultimate strength of the tested specimens. Afterwards, the predicted capacities were compared with the tested results. Design codes present different expression for predicting ultimate strength. However, these strength predictors express the steel and concrete contribution of the CFST column. In design calculations, reduction factors or material safety factors are

set to unit. In order to determine the error of the predicted capacity, the experimental results were divided by the predicted results.

5.7.1 **Eurocode 4 (2005)**

The experimental ultimate loads were compared to the maximum loads calculated according to the design method proposed by EC4 (2005) for composite members. EC4 (2005) uses a different model in function of the cross-sectional shape. For rectangular sections, the capacity of the column is obtained as the sum of the contributions of each material. The results obtained by this method are summarized in Table 5.4 together with the error calculated with respect to the experimental values. As can be seen in Figure 5.1, EC4 produces in general unsafe predictions with a mean of 1.08.

Table 5.4 Code calculation results of Eurocode 4

| Symbol	B x t x L	f_c'	f_y	B/t	L/B	P_{exp}	P_{EC4}	P_{EC4} / P_{exp}
	(mm x mm x mm)	(Mpa)	(MPa)			(kN)	(kN)	
C1	100 x 4 x 1000	27	350	25	10	697	757	1.09
C2	100 x 4 x 1000	35	350	25	10	729	821	1.13
C3	100 x 4 x 1000	44	350	25	10	804	900	1.12
C4	125 x 3 x 1000	35	350	41.6	8	930	998	1.07
C5	125 x 4 x 1000	35	350	31.2	8	1011	1146	1.12
C6	125 x 5 x 1000	35	350	25	8	1269	1269	1.00
C7	100 x 4 x 500	35	350	25	5	770	821	1.06
C8	100 x 4 x 300	35	350	25	3	810	821	1.01
C9	150 x 4 x 1000	35	350	37.5	6.6	1340	1508	1.13
							Mean	1.08
							Standard deviation	0.05
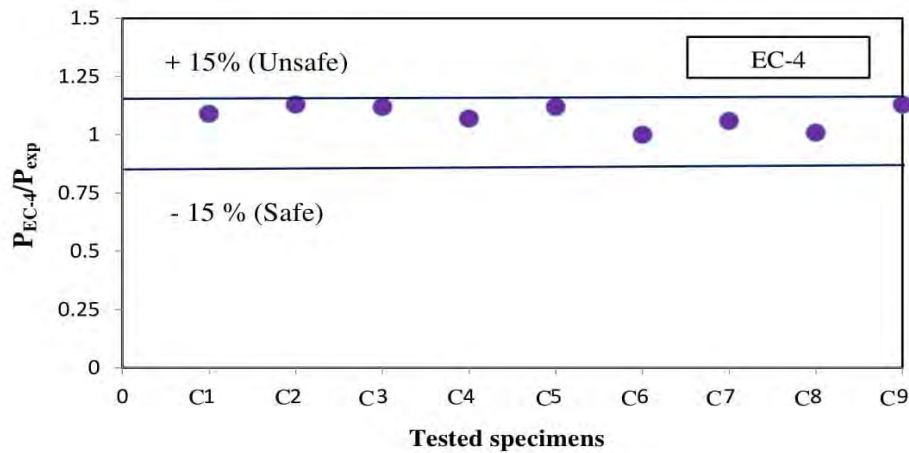
Figure 5.1 Comparison between the predicted (EC-4) and measured strength.

5.7.2 ACI-318 (2014) Code

This formula does not differentiate between different cross-sectional shapes. In general, ACI (2014) code predicts the ultimate strength with good prediction accuracy. The predicted axial strength for each specimen is given in Table 5.5. The graphical representation of this data is displayed in Figure 5.2. Where the average P_{ACI} / P_{exp} ratio is 1.02 with a standard deviation of 0.04. In addition, the prediction accuracy of the ACI is more accurate than that of EC4, where the average P_{EC4} / P_{exp} ratio is 1.08.

Table 5.5 Code calculation results of ACI-318

| Symbol	B x t x L	$f_c^{/}$	f_y	B/t	L/B	P_{exp}	P_{ACI}	P_{ACI} / P_{exp}
	(mm x mm x mm)	(Mpa)	(MPa)			(kN)	(kN)	
C1	100 x 4 x 1000	27	350	25	10	697	724	1.04
C2	100 x 4 x 1000	35	350	25	10	729	777	1.07
C3	100 x 4 x 1000	44	350	25	10	804	865	1.07
C4	125 x 3 x 1000	35	350	41.6	8	930	960	1.03
C5	125 x 4 x 1000	35	350	31.2	8	1011	1074	1.05
C6	125 x 5 x 1000	35	350	25	8	1269	1201	0.95
C7	100 x 4 x 500	35	350	25	5	770	777	1.00
C8	100 x 4 x 300	35	350	25	3	810	777	0.95
C9	150 x 4 x 1000	35	350	37.5	6.6	1340	1403	1.05
							Mean	1.02
							Standard deviation	0.04
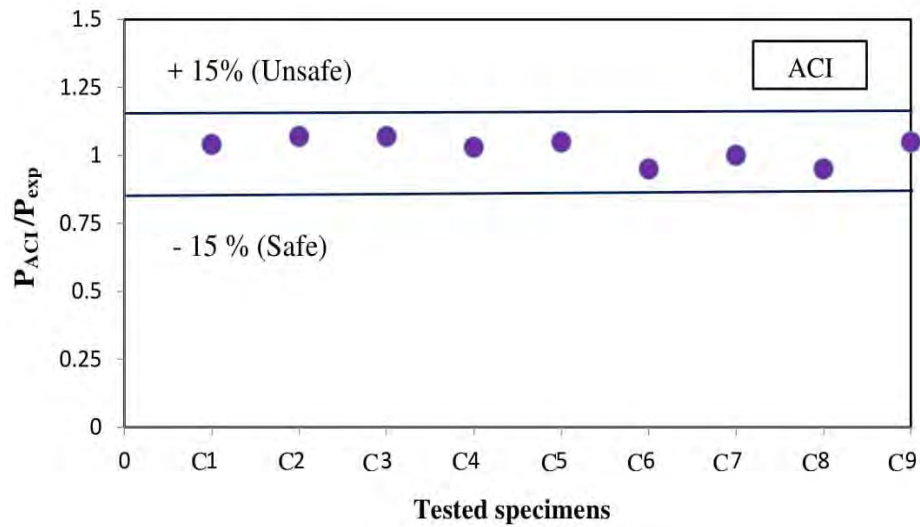
Figure 5.2 Comparison between the predicted (ACI-318) and measured strength.

5.7.3 **American Institute of Steel Construction (AISC)**

AISC (2010) composite column design presents different equations for the cross-sectional strength depending on the shape of the column and the ratio maximum dimension to thickness. Besides, the expression for the nominal axial capacity of stub columns incorporates the effect of slenderness. AISC (2010) presented best prediction with a mean of 1.01 and Standard deviation of 0.03.The predictions given by this method are shown in Table 5.6 and Figure 5.3.

Table 5.6 Code calculation results of AISC

| Symbol	B x t x L	$f_c^/$	f_y	B/t	L/B	P_{exp}	P_{AISC}	P_{AISC} / P_{exp}
	(mm x mm x mm)	(Mpa)	(MPa)			(kN)	(kN)	
C1	100 x 4 x 1000	27	350	25	10	697	687	0.99
C2	100 x 4 x 1000	35	350	25	10	729	736	1.01
C3	100 x 4 x 1000	44	350	25	10	804	798	0.99
C4	125 x 3 x 1000	35	350	41.6	8	930	890	0.95
C5	125 x 4 x 1000	35	350	31.2	8	1011	1037	1.02
C6	125 x 5 x 1000	35	350	25	8	1269	1160	0.91
C7	100 x 4 x 500	35	350	25	5	770	767	0.99
C8	100 x 4 x 300	35	350	25	3	810	774	0.95
C9	150 x 4 x 1000	35	350	37.5	6.6	1340	1368	1.02
							Mean	0.99
							Standard deviation	0.04
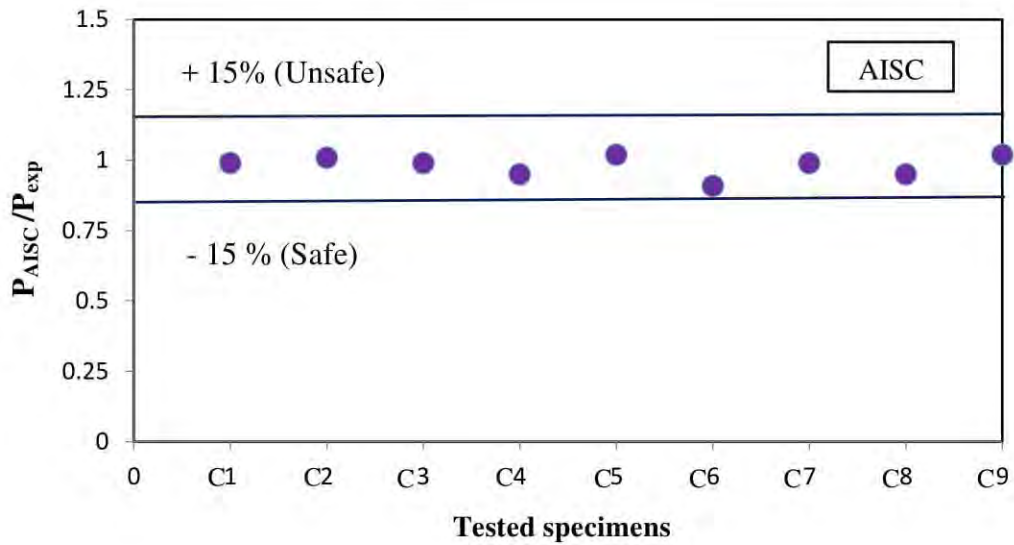
Figure 5.3 Comparison between the predicted (AISC) and measured strength.

5.7.4 Wang et al. (2016) Formulae

The predictions given by this method are shown in Table 5.7 and Figure 5.4 and are in general unsafe, particularly for square and rectangular columns. They produce an unsafe mean with the highest value (1.12) of all the methods analyzed.

Table 5.7 Code calculation results of Wang et al. (2016)

Symbol	B x t x L	$f_c^{/}$	f_y	B/t	L/B	P_{exp}	$P_{Wang\ et\ al.}$	$P_{Wang\ et\ al.}$ / P_{exp}
	(mm x mm x mm)	(Mpa)	(MPa)			(kN)	(kN)	
C1	100 x 4 x 1000	27	350	25	10	697	802	1.15
C2	100 x 4 x 1000	35	350	25	10	729	861	1.18
C3	100 x 4 x 1000	44	350	25	10	804	930	1.15
C4	125 x 3 x 1000	35	350	41.6	8	930	1010	1.08
C5	125 x 4 x 1000	35	350	31.2	8	1011	1180	1.16
C6	125 x 5 x 1000	35	350	25	8	1269	1345	1.05
C7	100 x 4 x 500	35	350	25	5	770	861	1.11
C8	100 x 4 x 300	35	350	25	3	810	861	1.06
C9	150 x 4 x 1000	35	350	37.5	6.6	1340	1537	1.14
							Mean	1.12
							Standard deviation	0.04
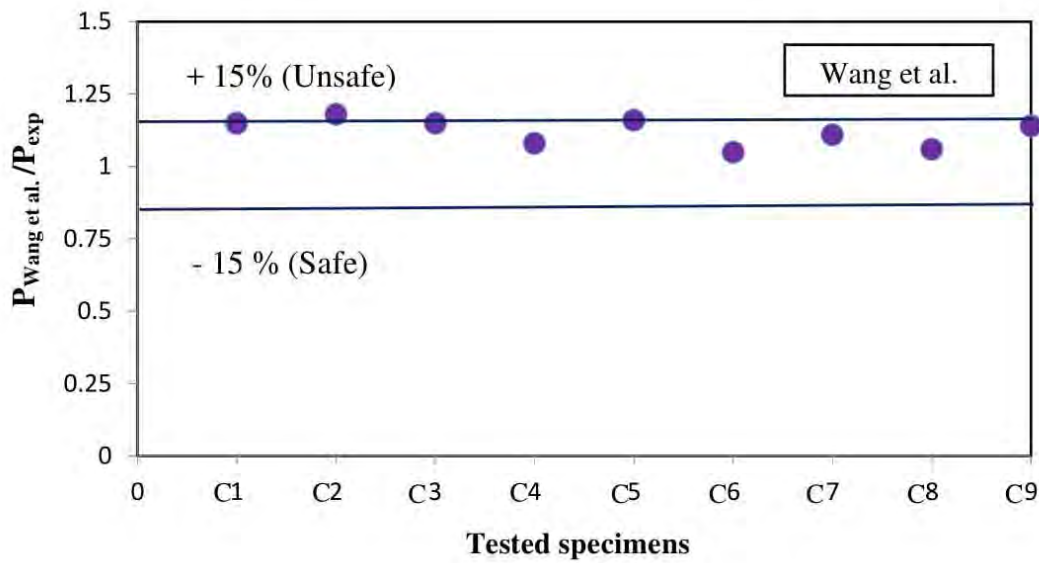
Figure 5.4 Comparison between the predicted (Wang et al. 2016) and measured strength.

5.8   Summary

All the codes somewhat overestimated the capacities except AISC(2010). AISC presented best prediction with a mean of 0.99 and Standard deviation of 0.04. EC4 (2005) and ACI (2014) predicted higher capacity than the experimental results about 8% and 2% respectively; whilst Wang et al. (2016) predicted highest 12% higher capacity of all the methods analyzed. In general, all the codes showed good agreement with the experimental results.

CHAPTER 6
CONCLUSIONS AND RECOMMENDATIONS

6.1   General conclusions

In this study nine square CFST columns with a variety of geometric and material properties were tested under axial compression. The tested columns were filled by concrete with compressive strength of 27 MPa to 44 MPa, cross-sectional slenderness ratio of 25 to 42 and global slenderness ratio of 3 to 10. The influence of these parameters on the failure mode, load-strain response, ultimate load and performance indexes of the square CFST columns were investigated. Finally, the design approaches adopted in (Eurocode 4, AISC-LRFD 2010, ACI 2014 and Wang et al. 2016) were reviewed and applied to calculate the ultimate strength of the tests columns. Subsequently, the predicted values were compared with the experimental results obtained from the experiments. The following conclusions can be drawn within the limited scope of this study:

i.   The typical failure mode of the specimen was characterized by local buckling of the steel tube and crushing of concrete, but the failure of the specimens with L/B$\geq$10 exhibited global buckling. Specimens with higher cross-sectional width showed more pronounced outward buckling.

ii. Stiffness, ultimate capacity and concrete contribution ratio of the tested column decreased with the increase of cross-sectional width by tube thickness (B/t) ratio, whilst they increased with the increase of concrete compressive strength and the decrease of L/B ratio of the specimen.

iii. Axial strain at peak load, ductility and strength index of the tested specimen increased with the decrease of B/t ratio, concrete compressive strength and L/B ratio of the specimen.

iv. For teted columns, the positive effect of the confinement is not observed and the theoretical sectional capacity overestimated the real capacity. To overcome this problem a strength reduction factor may be included in the design codes of square CFST column.

v.   The codes somewhat overestimated the ultimate load except AISC(2010), having lower difference between the predicted and experimental results.

AISC (2010) presented best prediction with a mean of 0.99 and Standard deviation of 0.04.

6.2   Future recommendations

The tests reported as part of this study concentrated on the ultimate load capacity and load-displacement relationships of CFST columns. In order to derive constitutive models for determining the properties of such columns, detailed examination of the longitudinal and transverse load-strain relationships for all parametric ranges are required. It is considered that in further research studies, the following aspects should be given special attention:

i. The volumetric expansion of the confined concrete and the effective stresses which develop in the steel tube for CFST columns utilizing high strength concrete and high strength steel.

ii. The stress-strain relationship of CFST columns and the effective stiffness of the composite sections.

iii. Proceeding assessment of the behavior of the CFST column under isolated conditions, studies should be extended to account for the eccentrically loaded columns and the application of CFST columns as frame elements.

iv. The effects of local buckling on column sections with D/t ratio which exceed current specified limits given in design standards.

References

ACI 318R (2014), "Building Code Requirements for Structural Concrete". American Concrete Institute, ACI, Detroit.

AIJ (2008). "Recommendations for design and construction of concrete filled steel tubular structures". Architectural Institute of Japan, Tokyo, Japan.

AISC-LRFD (2010), "AISC Manual for Steel Construction". American Institute for Steel Construction, USA.

AS5100 (2004), "Bridge Design-steel and Composite Construction". Australian Standard.

ASTM D638-02a (2003), "Standard test method for tensile properties of plastics". American Society of Testing Materials.

Bergmann, R. (1994). "Load Introduction in Composite Columns Filled With High Strength Concrete," Tubular Structures VI, Proceedings of the Sixth International Symposium on Tubular Structures, 373-380.

BNBC (2016), "Bangladesh National Building Code". Dhaka, Draft version.

CSA Standard S16 (2009), "Design of steel structures". Published by Canadian Standards Association, A not-for-profit private sector organization 5060 Spectrum Way, Suite 100, Mississauga, Ontario, Canada.

DBJ/T 13-51-2010 2010. Technical specification for concrete-filled steel tubular structures. Department of Housing and Urban-Rural Development of Fujian Province, Fuzhou, China.

European Committee for Standardization (1994). "Eurocode 4: Design of Composite Steel and Concrete Structures". CEN.

FU, Z. Q., JI, B. H., LV, L. & ZHOU, W. J. (2011). " Behaviour of lightweight aggregate concrete filled steel tubular slender columns under axial compression". *Advanced Steel Construction*, 7(2), 144–156.

FU, Z. Q., JI, B. H., ZHOU, Y. & WANG, X. L. (2011). "An Experimental Behavior of Lightweight Aggregate Concrete Filled Steel Tubular Stub under Axial Compression". In: *GeoHunan International Conference 2011*, 24–32.

Gabel, R. J., Carver, R. M., and Gerometta, M. (2015). "The Skyscraper Surge Continues in 2015, The 'Year of 100 Supertalls.'" 10.

Giakoumelis, G. and Lam, D. (2003). "Axial Capacity of Circular Concrete-Filled Tube Columns," Journal of Constructional Steel Research, 60, 1049-1068.

Guo, L., Zhang, S., Kim, W.-J., and Ranzi, G. (2007). "Behavior of square hollow steel tubes and steel tubes filled with concrete." Thin-Walled Structures, 45(12), 961-973.

Han, L.-H., Li, W., and Bjorhovde, R. (2014). "Developments and advanced applications of concrete-filled steel tubular (CFST) structures: Members." *Journal of Constructional Steel Research*, 100, 211–228.

HAN, L. H., REN, Q. X. & LI, W. (2010). "Tests on inclined, tapered and STS concrete-filled steel tubular (CFST) stub columns". *Journal of Constructional Steel Research*, 66(10), 1186–1195.

Han, L.-H. and Yan, S.-Z. (2000). "Experimental Studies on the Strength with High Slenderness Ratio Concrete Filled Steel Tubular Columns," Composite and Hybrid Structures, Proceedings of the Sixth ASCCS International Conference on Steel-Concrete Composite Structures, 419-426.

Ibañez, C., Hernández-Figueirido, D., and Piquer, A. (2018). "Shape effect on axially loaded high strength CFST stub columns." *Journal of Constructional Steel Research*, 147, 247–256.

Johansson, M. and Gylltoft, K. (2002). " Mechanical Behavior of Circular Steel-Concrete Composite Stub Columns," Journal of Structural Engineering, ASCE, 128(8), 1073-1081.

Kitada, T., Yoshida, Y., and Nakai, H. (1987). "Fundamental Study on Elastoplastic Behavior of Concrete Encased Steel Short Tubular Columns," Memoirs of the Faculty of Engineering, Osaka City University, Osaka, Japan, 28, 237-253.

Klöppel, K. and Goder, W. (1957). "Traglastversuche mit ausbetonierten Stahlrohen und Aufstellung einer Bemessungsformel," Der Stahlbau, Berlin, 26, No. 1, January 1957.

Knowles, R. B. and Park, R. (1969). "Strength of Concrete Filled Steel Tubular Columns," Journal of the Structural Division, ASCE, 95, 2565-2587.

LI, W., REN, Q. X., HAN, L. H. & ZHAO, X. L. (2012). " Behaviour of tapered concrete-filled double skin steel tubular (CFDST) stub columns." *Thin-Walled Structures*, 57, 37–48.

Liang, Q. Q., Patel, V. I., and Hadi, M. N. S. (2012). "Biaxially loaded high-strength concrete-filled steel tubular slender beam-columns, Part I: Multiscale simulation." *Journal of Constructional Steel Research*, 75, 64–71.

Luksha, L. K., and Nesterovich, A. P. (1991). "Strength of Tubular Concrete Cylinders under Combined Loading." Proceedings of 3rd International Conference on Steel-Concrete Composite Structures, Fukuoka, Japan, 67–71.

Mahgub, M., Ashour, A., Lam, D., and Dai, X. (2017). "Tests of self-compacting concrete filled elliptical steel tube columns." *Thin-Walled Structures*, 110, 27–34.

Masuo, K., Adachi, M., Kawabata, K., Kobayashi, M., and Konishi, M. (1991). "Buckling Behavior of Concrete Filled Circular Steel Tubular Columns Using Light-Weight Concrete," Proceedings of the Third International Conference on Steel-Concrete Composite Structures, 95-100.

MURSI, M. & UY, B. (2004). "Strength of slender concrete filled high strength steel box columns." *Journal of Constructional Steel Research*, 60(12), 1825–1848.

O'Shea, M. D. and Bridge, R. Q. (1994). "Tests of Thin-Walled Concrete-Filled Steel Tubes," Preliminary Report, Center for Advanced Structural Engineering, University of Sydney, Australia.

O'Shea, M. D. and Bridge, R. Q. (1997). "Behaviour of Thin-Walled Box Sections with Lateral Restraint," Research Report No. R739, School of Civil Engineering, University of Sydney, Sydney, Australia, March.

Portolés, J. M., Romero, M. L., Bonet, J. L., and Filippou, F. C. (2011). "Experimental study of high strength concrete-filled circular tubular columns under eccentric loading." *Journal of Constructional Steel Research*, 67(4), 623–633.

Ren, Q.-X., Zhou, K., Hou, C., Tao, Z., and Han, L.-H. (2018). "Dune sand concrete-filled steel tubular (CFST) stub columns under axial compression: Experiments." *Thin-Walled Structures*, 124, 291–302.

Sakino, K., Nakahara, H., Morino, S., and Nishiyama, I. (2004). "Behavior of Centrally Loaded Concrete-Filled Steel-Tube Short Columns." *Journal of Structural Engineering*, 130(2), 180–188.

SCHNEIDER, S. P. (1998). "Axially loaded concrete-filled steel tubes". *Journal of Structural Engineering*, 124(10), 1125–1138.

Shanmugam, N. E., and Lakshmi, B. (2001). "State of the art report on steel–concrete composite columns." *Journal of Constructional Steel Research*, 57(10), 1041–1080.

Susantha, K. A. S., Ge, H., and Usami, T. (2001). "A CAPACITY PREDICTION PROCEDURE FOR CONCRETE-FILLED STEEL COLUMNS." *Journal of Earthquake Engineering*, 5(4), 483–520.

TAM, V. W., WANG, Z. B. & TAO, Z. (2014). " Behaviour of recycled aggregate concrete filled stainless steel stub columns". *Materials and Sructures*, 47(1), 293–310.

TAO, Z., HAN, L. H. & WANG, Z. B. (2005). "Experimental behaviour of stiffened concrete-filled thin-walled hollow steel structural (HSS) stub columns". *Journal of Constructional Steel Research*, 61(7), 962–983.

TAO, Z., HAN, L. H. & ZHAO, X. L. (2004). " Behaviour of concrete-filled double skin (CHS inner and CHS outer) steel tubular stub columns and beam-columns". *Journal of Constructional Steel Research*, 60(8), 1129–1158.

Shakir-Khalil, H. and Zeghiche, Z. (1989). "Experimental Behavior of Concrete-Filled Rolled Rectangular Hollow-Section Columns." The Structural Engineer, 67(19), 345-353.

Tsuda, K., Matsui, C., and Mino, E. (1996). "Strength and Behavior of Slender Concrete Filled Steel Tubular Columns," Stability Problems in Designing, Construction and Rehabilitation of Metal Structures, Proccedings of the Fifth International Colloquium on Structural Stability, 489-500.

UY, B. (2001). "Strength of short concrete filled high strength steel box columns. " *Journal of Constructional Steel Research*, 57(2), 113–134.

Uy, B. (2008). "Stability and ductility of high performance steel sections with concrete infill." *Journal of Constructional Steel Research*, 64(7–8), 748–754.

Uy, B., Tao, Z., and Han, L.-H. (2011). "Behaviour of short and slender concrete-filled stainless steel tubular columns." *Journal of Constructional Steel Research*, 67(3), 360–378.

VARMA, A. H., RICLES, J. M., SAUSE, R. & LU, L. W. (2002). "Experimental behavior of high strength square concrete-filled steel tube beam-columns. " *Journal of Structural Engineering*, 128(3), 309–318.

Xiamuxi, A., and Hasegawa, A. (2012). "A study on axial compressive behaviors of reinforced concrete filled tubular steel columns." *Journal of Constructional Steel Research*, 76, 144–154.

XIONG, D. X. (2012). "Structural behaviour of concrete filled steel tubes with high strength materials. " *PhD thesis*, National University of Singapore.

YANG, Y. F. & HAN, L. H. (2006). "Experimental behaviour of recycled aggregate concrete filled steel tubular columns." *Journal of Constructional Steel Research*, 62(12), 1310–1324.

YOUNG, B. & ELLOBODY, E. (2006). "Experimental investigation of concrete-filled cold-formed high strength stainless steel tube columns." *Journal of Constructional Steel Research*, 62(5), 484–492.

YU, Q., TAO, Z. & WU, Y. X. (2008). " Experimental behaviour of high performance concrete-filled steel tubular columns. " *Thin-Walled Structures*, 46(4), 362–370.

Zeghiche, J., and Chaoui, K. (2005). "An experimental behaviour of concrete-filled steel tubular columns." *Journal of Constructional Steel Research*, 61(1), 53–66.

Zhang, S. and Zhou, M. (2000). "Stress-Strain Behavior of Concrete-Filled Square Steel Tubes," Composite and Hybrid Structures, Proceedings of the Sixth ASCCS International Conference on Steel-Concrete Composite Structures, 403-409.

ZHAO, X. L. & GRZEBIETA, R. (2002). "Strength and ductility of concrete filled double skin (SHS inner and SHS outer) tubes". *Thin-Walled Structures*, 40(2), 199–213.

Zhao, XL, Han, LH & Lu, H (2010). "Concrete-filled tubular members and connections", Spon Press London.

Zhong, S.-T. and Miao, R.-Y. (1988). "Stress-Strain Relationship and Strength of Concrete Filled Tubes," Composite Construction in Steel and Concrete, Proceedings of the Engineering Foundation Conference, 773-785.

Zhu, M., Liu, J., Wang, Q., and Feng, X. (2010). "Experimental research on square steel tubular columns filled with steel-reinforced self-consolidating high-strength concrete under axial load." *Engineering Structures*, 32(8), 2278–2286.